enhanced actin polymerization, altered cytoskeletal responses, and genomic instability in lymphocytes. *J. Exp. Med.* 207:1145.
17 Kim, A. S., Kakalis, L. T., Abdul-Manan, N., Liu, G. A. and Rosen, M. K. 2000. Autoinhibition and activation mechanisms of the Wiskott-Aldrich syndrome protein. *Nature* 404:151.
18 Badour, K., Zhang, J., Shi, F., Leng, Y., Collins, M. and Siminovitch, K. A. 2004. Fyn and PTP-PEST-mediated regulation of Wiskott-Aldrich syndrome protein (WASp) tyrosine phosphorylation is required for coupling T cell antigen receptor engagement to WASp effector function and T cell activation. *J. Exp. Med.* 199:99.
19 Torres, E. and Rosen, M. K. 2003. Contingent phosphorylation/dephosphorylation provides a mechanism of molecular memory in WASP. *Mol. Cell* 11:1215.
20 Torres, E. and Rosen, M. K. 2006. Protein-tyrosine kinase and GTPase signals cooperate to phosphorylate and activate Wiskott-Aldrich syndrome protein (WASP)/neuronal WASP. *J. Biol. Chem.* 281:3513.
21 Wu, X., Suetsugu, S., Cooper, L. A., Takenawa, T. and Guan, J. L. 2004. Focal adhesion kinase regulation of N-WASP subcellular localization and function. *J. Biol. Chem.* 279:9565.
22 Westphal, R. S., Soderling, S. H., Alto, N. M., Langeberg, L. K. and Scott, J. D. 2000. Scar/WAVE-1, a Wiskott-Aldrich syndrome protein, assembles an actin-associated multi-kinase scaffold. *EMBO J.* 19:4589.
23 Miki, H., Miura, K. and Takenawa, T. 1996. N-WASP, a novel actin-depolymerizing protein, regulates the cortical cytoskeletal rearrangement in a PIP2-dependent manner downstream of tyrosine kinases. *EMBO J.* 15:5326.
24 Wu, X., Yoo, Y., Okuhama, N. N., Tucker, P. W., Liu, G. and Guan, J. L. 2006. Regulation of RNA-polymerase-II-dependent transcription by N-WASP and its nuclear-binding partners. *Nat. Cell Biol.* 8:756.
25 Taylor, M. D., Sadhukhan, S., Kottangada, P. *et al.* 2010. Nuclear role of WASp in the pathogenesis of dysregulated TH1 immunity in human Wiskott-Aldrich syndrome. *Sci. Transl. Med.* 2:37ra44.
26 Suetsugu, S. and Takenawa, T. 2003. Translocation of N-WASP by nuclear localization and export signals into the nucleus modulates expression of HSP90. *J. Biol. Chem.* 278:42515.
27 Rawe, V. Y., Payne, C., Navara, C. and Schatten, G. 2004. WAVE1 intranuclear trafficking is essential for genomic and cytoskeletal dynamics during fertilization: cell-cycle-dependent shuttling between M-phase and interphase nuclei. *Dev. Biol.* 276:253.
28 Görlich, D. and Mattaj, I. W. 1996. Nucleocytoplasmic transport. *Science* 271:1513.
29 Cory, G. O., Garg, R., Cramer, R., and Ridley, A. J. 2002. Phosphorylation of tyrosine 291 enhances the ability of WASp to stimulate actin polymerization and filopodium formation. *J. Biol. Chem.* 277:45115.
30 Dovas, A. and Cox, D. 2010. Regulation of WASp by phosphorylation: activation or other functions? *Commun. Integr. Biol.* 3:101.
31 Snapper, S. B., Takeshima, F., Antón, I. *et al.* 2001. N-WASP deficiency reveals distinct pathways for cell surface projections and microbial actin-based motility. *Nat. Cell Biol.* 3:897.
32 Shav-Tal, Y. and Zipori, D. 2002. PSF and p54(nrb)/NonO–multifunctional nuclear proteins. *FEBS Lett.* 531:109.
33 Kameoka, S., Duque, P. and Konarska, M. M. 2004. p54(nrb) associates with the 5' splice site within large transcription/splicing complexes. *EMBO J.* 23:1782.
34 Kroft, S. H., Finn, W. G., Singleton, T. P., Ross, C. W., Sheldon, S. and Schnitzer, B. 1998. Follicular large cell lymphoma with immunoblastic features in a child with Wiskott-Aldrich syndrome: an unusual immunodeficiency-related neoplasm not associated with Epstein-Barr virus. *Am. J. Clin. Pathol.* 110:95.
35 Kawakami, K., Yamaguchi, M., Watanabe, Y. and Murata, T. 2002. Development of diffuse large cell lymphoma from follicular lymphoma with multiple immunoglobulin heavy chain gene rearrangement occurring in a patient with Wiskott-Aldrich syndrome. *Int. J. Hematol.* 76:196.
36 Du, S., Scuderi, R., Malicki, D. M., Willert, J., Bastian, J. and Weidner, N. 2011. Hodgkin's and non-Hodgkin's lymphomas occurring in two brothers with Wiskott-Aldrich syndrome and review of the literature. *Pediatr. Dev. Pathol.* 14:64.
37 Moulding, D. A., Blundell, M. P., Spiller, D. G. *et al.* 2007. Unregulated actin polymerization by WASp causes defects of mitosis and cytokinesis in X-linked neutropenia. *J. Exp. Med.* 204:2213.

T-cell receptor ligation causes Wiskott-Aldrich syndrome protein degradation and F-actin assembly downregulation

Yuko Watanabe, MD, PhD,[a]* Yoji Sasahara, MD, PhD,[a]* Narayanaswamy Ramesh, PhD,[b]* Michel J. Massaad, PhD,[b]* Chung Yeng Looi, PhD,[a] Satoru Kumaki, MD, PhD,[a] Shigeo Kure, MD, PhD,[a] Raif S. Geha, MD,[b]‡ and Shigeru Tsuchiya, MD, PhD[a]‡ *Miyagi, Japan, and Boston, Mass*

Background: Wiskott-Aldrich syndrome protein (WASP) links T-cell receptor (TCR) signaling to the actin cytoskeleton. WASP is normally protected from degradation by the Ca^{++}-dependent protease calpain and by the proteasome because of its interaction with the WASP-interacting protein.
Objective: We investigated whether WASP is degraded after TCR ligation and whether its degradation downregulates F-actin assembly caused by TCR ligation.
Methods: Primary T cells, Jurkat T cells, and transfected 293T cells were used in immunoprecipitation experiments. Intracellular F-actin content was measured in splenic T cells from wild-type, WASP-deficient, and c–Casitas B-lineage lymphoma (Cbl)-b–deficient mice by using flow cytometry. Calpeptin and MG-132 were used to inhibit calpain and the proteasome, respectively.
Results: A fraction of WASP in T cells was degraded by calpain and by the ubiquitin-proteasome pathway after TCR ligation. The Cbl-b and c-Cbl E3 ubiquitin ligases associated with WASP after TCR signaling and caused its ubiquitination. Inhibition of calpain and lack of Cbl-b resulted in a significantly more sustained increase in F-actin content after TCR ligation in wild-type T cells but not in WASP-deficient T cells.
Conclusion: TCR ligation causes WASP to be degraded by calpain and to be ubiquitinated by Cbl family E3 ligases, which targets it for destruction by the proteasome. WASP degradation might provide a mechanism for regulating WASP-dependent TCR-driven assembly of F-actin. (J Allergy Clin Immunol 2013;132:648-55.)

Key words: *Wiskott-Aldrich syndrome, Wiskott-Aldrich syndrome protein, T-cell receptor, calpain, ubiquitination, proteasome, F-actin, Cbl family proteins*

Abbreviations used
Arp: Actin-related protein
Cbl: Casitas B-lineage lymphoma
EVH1: Ena-VASP homology domain 1
IS: Immune synapse
TCR: T-cell receptor
WAS: Wiskott-Aldrich syndrome
WASP: Wiskott-Aldrich syndrome protein
WIP: WASP-interacting protein
WT: Wild-type
ZAP-70: ζ Chain–associated protein kinase of 70 kDa

Wiskott-Aldrich syndrome (WAS) is an X-linked recessive disorder characterized by variable immunodeficiency, eczema, and thrombocytopenia.[1] The gene for Wiskott-Aldrich syndrome protein (WASP) is mutated in patients with WAS and X-linked thrombocytopenia. *WAS* is located on Xp11.22-p11.23 and encodes a protein of 502 amino acids and approximately 60 kDa in molecular weight.[2,3] WASP expression is restricted to hematopoietic cells.[3]

WASP has an N-terminal Ena/VASP homology domain 1 (EVH1) domain, a Cdc42/Rac GTPase-binding domain, a proline-rich domain, a G actin–binding verprolin homology (V) domain, a cofilin homology (C) domain, and a C-terminal acidic (A) segment.[1] The last 3 domains are located at the C-terminal end of WASP and are collectively referred to as the VCA domain. WASP interacts with WASP-interacting protein (WIP) through its EVH1 domain; with Cdc42-GTP through its GTPase-binding domain; with multiple SH3 domain–containing proteins, which include Nck, Grb2, and cortactin, through its proline-rich region; and with the actin-related protein (Arp) 2/3 complex that initiates actin polymerization through its VCA domain.[4-6]

WASP plays a critical role in T-cell activation and actin reorganization.[7-9] T cells from patients with WAS and $WASP^{-/-}$ mice are deficient in their ability to increase their F-actin content, secrete IL-2, and proliferate after T-cell receptor (TCR) ligation.[10-12] WASP exists in cells in a closed inactive conformation through intramolecular interactions that prevent the VCA domain from activating the Arp2/3 complex. Binding of Cdc42-GTP or of the SH3 domain of adaptor proteins, as well as phosphorylation of tyrosine (Y) at position 291, is thought to cause a conformational change in WASP, which allows the VCA domain to interact with and activate the Arp2/3 complex.[5,13-15] The WASP-interacting protein (WIP) is expressed at high levels in lymphoid tissues. Most of WASP is associated with WIP in T cells.[16] WIP binds through its C-terminal end to the EVH1 domain of WASP. WIP plays an important role in the recruitment of the WASP-WIP complex to ζ chain–associated protein kinase of 70 kDa (ZAP-70) and

From [a]the Department of Pediatrics, Tohoku University Graduate School of Medicine, Miyagi, and [b]the Division of Immunology, Children's Hospital, and the Department of Pediatrics, Harvard Medical School, Boston.
*These authors contributed equally to this work.
‡These authors contributed equally as senior authors.
Supported by grants-in-aid from the Japan Ministry of Education, Culture, Sports, Science and Technology and a grant for research on intractable diseases from the Japan Ministry of Health, Labour and Welfare (to Y.S. and S.T.), grants from the Japan Foundation for Pediatric Research and the Mother and Child Health Foundation (to Y.S.) and by US Public Health Service grant HL059561.
Disclosure of potential conflict of interest: The authors have been supported by one or more grants from the National Institutes of Health.
Received for publication January 9, 2013; revised March 28, 2013; accepted for publication March 29, 2013.
Available online May 16, 2013.
Corresponding author: Yoji Sasahara, MD, PhD, Department of Pediatrics, Tohoku University Graduate School of Medicine, 1-1 Seiryo-machi, Aoba-ku, Sendai, Miyagi 980-8574, Japan. E-mail: ysasahara@med.tohoku.ac.jp.
0091-6749/$36.00

http://dx.doi.org/10.1016/j.jaci.2013.03.046

to the immunologic synapse after TCR ligation.[17] More importantly, WIP stabilizes WASP in T cells. This is evidenced by the finding that WASP levels are significantly reduced in T cells from $WIP^{-/-}$ mice and a WIP-deficient patient.[16,18] Furthermore, most missense mutations in WASP that result in diminished WASP levels are localized to the WIP-binding EVH1 domain of WASP and disrupt the WASP-WIP interaction.[19,20] Expression of the WASP-binding domain of WIP in these cells restores WASP levels close to normal.[21] Treatment with calpain and proteasome inhibitors increases WASP protein levels in T cells from $WIP^{-/-}$ mice and patients with WAS with missense mutations that disrupt WIP binding,[16] indicating that WASP can be subject to degradation by calpain and the ubiquitin-proteasome pathway.

Unregulated activation of WASP is detrimental to many cell types, especially cells of the myeloid lineage. Three different mutations of WASP, namely L270P, S272P, and I294T, destroy the autoinhibitory conformation of WASP, resulting in a constitutively active protein, and cause X-linked neutropenia.[22] The L270P and S272P mutations localize to the GTPase-binding domain,[23] whereas the I294T mutation is located close to the tyrosine residue Y291, which, when phosphorylated, results in the activation of WASP.[24] Knock-in mouse models mimicking the L270P and I294T mutations have been described.[25] T and B cells from these mice show a marked increase in F-actin levels but migrate normally in response to chemokines.

In this study we demonstrate that TCR ligation causes WASP to be degraded by calpain and by Casitas B-lineage lymphoma (Cbl)–mediated ubiquitination and proteasomal destruction. We demonstrate that WASP degradation provides a mechanism for downregulating TCR-driven assembly of F-actin.

METHODS

Cell lines and T cells

Jurkat T cells were obtained from the American Type Culture Collection and maintained in RPMI medium (Gibco, Carlsbad, Calif) supplemented with 10% FBS. 293T cells were a gift from Dr N. Ishii (Tohoku University, Sendai, Japan) and were maintained in Dulbecco modified Eagle medium (Gibco) supplemented with 10% FBS. Spleens from Cbl-b knockout (*Cbl-b*$^{-/-}$) mice and genetically matched wild-type (WT) shipping controls were a generous gift from Dr H. Gu, Columbia University. WASP-deficient mice were obtained from Dr Scott Snapper. Splenic T cells were isolated by using T-cell enrichment columns (Miltenyi Biotec, Bergisch Gladbach, Germany).

Antibodies

Anti-WASP 5A5 mAb, which recognizes the epitope in the region corresponding to amino acids 146 to 265, was developed in our laboratory.[26] Anti-WASP rabbit polyclonal antibody K374 (a gift from Dr Ignacio Molina) is directed to the C-terminal 20 amino acids of WASP.[16] Anti–phospho-WASP antibody, which recognized WASP phosphorylated on Y291, was purchased from Abcam (Cambridge, United Kingdom). Anti-ubiquitin mAb P4D1, anti–c-Cbl mAb A-9, and anti–Cbl-b mAb G-1 were from Santa Cruz Biotechnology (Santa Cruz, Calif). Anti-actin mAb and anti-FLAG mAb were from Sigma (St Louis, Mo). Anti-HA mAb was from Cell signaling (Danvers, Mass). Control rabbit IgG was from Upstate (Billerica, Mass).

TCR stimulation, immunoprecipitation, and Western blotting

TCR ligation was performed, as described previously.[17] Briefly, T cells were incubated with 10 μg/mL anti-CD3 mAb UCHT1 (Calbiochem, San Diego, Calif) on ice for 20 minutes, followed by cross-linking with 15 μg/mL goat anti-mouse IgG (H+L; Caltag, Buckingham, United Kingdom) at 37°C for the indicated period. Cells were lysed in ice-cold lysis buffer containing 1% Triton X-100 and protease inhibitors. Cell lysates were clarified at 14,000*g* for 20 minutes at 4°C. For immunoprecipitation, cell lysates were precleared with protein G–Sepharose (GE Healthcare, Fairfield, Conn) for 2 hours and incubated overnight at 4°C with 4 μg of the indicated antibody preadsorbed onto protein G–Sepharose. Beads were washed 4 times with modified lysis buffer containing 0.2% Triton X-100. Bound proteins were eluted, run on 10% SDS-PAGE gels, and analyzed by means of Western blotting with the indicated antibodies followed by anti-mouse or anti-rabbit antibodies conjugated to horseradish peroxidase and enhanced chemiluminescent detection (Amersham Life Sciences, Piscataway, NJ). Densitometry was performed with CS Analyzer version 2.08 software (ATTO Corporation, Tokyo, Japan) or ImageJ version 1.45 software.

Calpain and proteasome inhibition

The proteasome inhibitor MG132 and the calpain inhibitor calpeptin were purchased from Calbiochem. Cells were cultured with calpeptin (1 μmol/L) or MG132 (10 μmol/L) for 6 hours before anti-CD3 stimulation.

Expression vectors and transfection

Human pcDNA3.1-EGFP-hWASP-WT was a generous gift from Dr K. A. Siminovitch (University of Toronto, Toronto, Ontario, Canada). Control pAcGFP1-C1 vector was purchased from Clontech (Mountain View, Calif). Human pcDNA3.1-3xFLAG-c-Cbl-WT, pcDNA3.1-3xFLAG-Cbl-b-WT, and pcDNA3.1-HA-Ub were gifts from Drs N. Ishii and Y. Tanaka (Tohoku University).[27] Control p3xFLAG-CMV-14 vector was purchased from Sigma. 293T cells were transiently transfected with lipofectamine, as described previously,[27] and harvested 48 hours after transfection.

Determination of cellular F-actin content

Flow cytometric analysis of F-actin content was performed, as described previously.[16] Briefly, mouse T cells were purified by using negative selection with the Pan T Cell Isolation Kit (Miltenyi Biotec) and then incubated for 6 hours with 1 μmol/L calpeptin. Cells were then washed and incubated with 10 μg/mL rat anti-mouse CD3 mAb (Serotec, Oxford, United Kingdom) for 30 minutes on ice. Cells were stimulated for the indicated times by cross-linking with goat anti-rat IgG (H+L) secondary antibody (Jackson Immunoresearch, West Grove, Pa). Cells were fixed in 4% formaldehyde, washed, and permeabilized with the CytoFix/CytoPerm cell staining kit (BD Biosciences, San Jose, Calif). F-actin was stained with tetramethylrhodamine isothiocyanate–labeled phalloidin (Invitrogen, Carlsbad, Calif). F-actin content was analyzed by measuring the mean fluorescent intensity with FACS LSRFortessa (Becton Dickinson) and FlowJo (TreeStar, Ashland, Ore) software.

Statistical analysis

Statistical analysis was performed with the Student *t* test.

RESULTS

WASP is C-terminally truncated by calpain after TCR ligation

Purified peripheral blood T cells were stimulated with anti-CD3 mAb followed by cross-linking with secondary antibody and cell lysates were immunoblotted for WASP to investigate whether WASP is degraded after TCR ligation. Immunoblotting with mAb 5A5, which recognizes an epitope in the region corresponding to amino acids 146 to 265, revealed a 62- to 64-kDa band in unstimulated T cells (Fig 1, *A*), as previously observed.[28] Stimulation with anti-CD3 resulted in the appearance of a 55-kDa

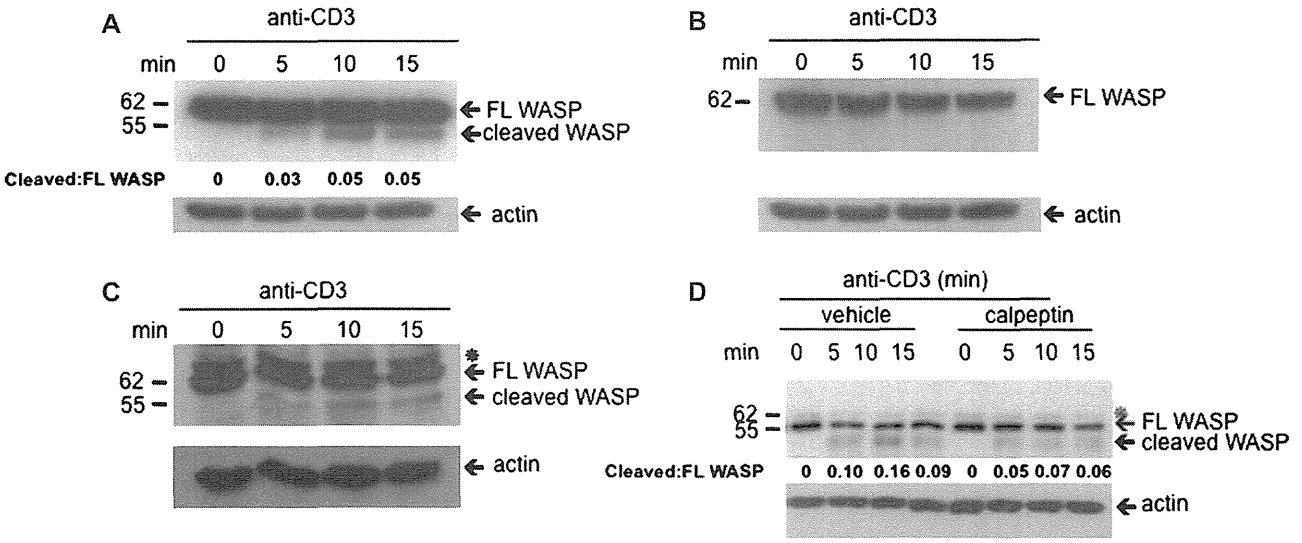

FIG 1. WASP is cleaved by calpain after TCR ligation. **A** and **B,** WASP immunoblot of peripheral blood T cells stimulated for 0 to 15 minutes with anti-CD3 mAb using mAb 5A5 (Fig 1, *A*) or polyclonal antibody K374 (Fig 1, *B*). **C,** WASP immunoblot of Jurkat T cells stimulated with anti-CD3 mAb using mAb 5A5. **D,** Effect of pretreatment for 6 hours with calpeptin on anti-CD3–driven WASP degradation in peripheral blood T cells. Lysates were immunoblotted with mAb 5A5. *Nonspecific band. The positions of molecular weight markers are indicated on the *left* in Fig 1, *A* to *D*. The ratio of cleaved WASP to full-length *(FL)* WASP in Fig 1, *A* and *D*, represents the mean of 5 experiments. Similar results were obtained in Fig 1, *A* to *D*, in 5 independent experiments.

WASP fragment at 5 minutes, which increased at 10 and 15 minutes after stimulation. Scanning densitometric analysis revealed that the intensity of the cleaved WASP band was approximately 5% that of the full-length WASP band at 10 and 15 minutes after stimulation. Similar results were obtained in Jurkat T cells (Fig 1, *C*).

Immunoblotting lysates of T cells with the rabbit polyclonal antibody K374 raised against the C-terminal 20 amino acids of WASP revealed the same 62- to 64-kDa band detected by using mAb 5A5 but did not detect the 55-kDa WASP fragment in anti-CD3–stimulated T cells that was detected by using mAb 5A5 (Fig 1, *B*). Similar results were obtained in Jurkat T cells (data not shown). This result indicates that the 55-kDa WASP fragment lacks the C-terminal VCA domains of WASP (amino acids 421-502) responsible for its actin-polymerizing activity.

Calpain cleaves WASP *in vitro*[29] and contributes to WASP degradation in WIP-deficient T cells.[16,30] To examine whether calpain was responsible for the cleavage of WASP after TCR ligation, T cells were pretreated with the calpain inhibitor calpeptin for 6 hours, washed, and stimulated with anti-CD3 mAb for 5 minutes. Preincubation with calpeptin attenuated by approximately 50% the generation of the 55-kDa WASP fragment in response to anti-CD3 stimulation (Fig 1, *D*), strongly suggesting that calpain mediates the C-terminal truncation of WASP after TCR/CD3 ligation, at least in part.

WASP is ubiquitinated and degraded by the proteasome in T cells after TCR ligation

In the absence of WIP, WASP is degraded by the ubiquitin-proteasome pathway.[16,30] To investigate whether WASP is a substrate for ubiquitination, we incubated *in vitro* transcribed and translated WASP with purified ubiquitin and ubiquitin-conjugating enzymes (mixture of E1, E2, and E3 enzymes), and the reaction mixture was immunoblotted with anti-ubiquitin mAb. WASP was polyubiquitinated in the presence of ubiquitin and ubiquitin-conjugating enzymes, as indicated by an intense high-molecular-weight smear (Fig 2, *A*). Addition of the 26S proteasome fraction to the ubiquitination mixture resulted in marked attenuation of the ubiquitinated WASP smear. These results indicate that after TCR/CD3 ligation, WASP is subject to ubiquitination, which targets it for destruction by the proteasome.

We next examined whether WASP is ubiquitinated in T cells after TCR ligation. Fig 2, *B*, shows the appearance of polyubiquitinated WASP after anti-CD3 mAb stimulation of Jurkat T cells. To examine whether WASP ubiquitinated after TCR ligation is targeted for destruction by the proteasome, Jurkat T cells were pretreated with the proteasome inhibitor MG132 for 6 hours and then stimulated with anti-CD3 mAb for 10 minutes, and WASP immunoprecipitates were prepared from their lysates and probed for ubiquitin. Fig 2, *C*, shows that ubiquitinated WASP was weakly detectable in unstimulated Jurkat cells, but its levels increased after TCR/CD3 stimulation. Pretreatment with MG132 modestly increased the amounts of ubiquitinated WASP in unstimulated Jurkat cells and strongly increased the amounts of ubiquitinated WASP detected after TCR/CD3 ligation. These results indicate that WASP is ubiquitinated and degraded by the proteasome after TCR ligation.

The Cbl family proteins c-Cbl and Cbl-b associate with WASP after TCR ligation and act as E3 ubiquitin ligases for WASP

Members of the Cbl family of E3 ubiquitin ligases are negative regulators in TCR signaling.[31,32] We tested the hypothesis that Cbl proteins might be involved in WASP ubiquitination. We first

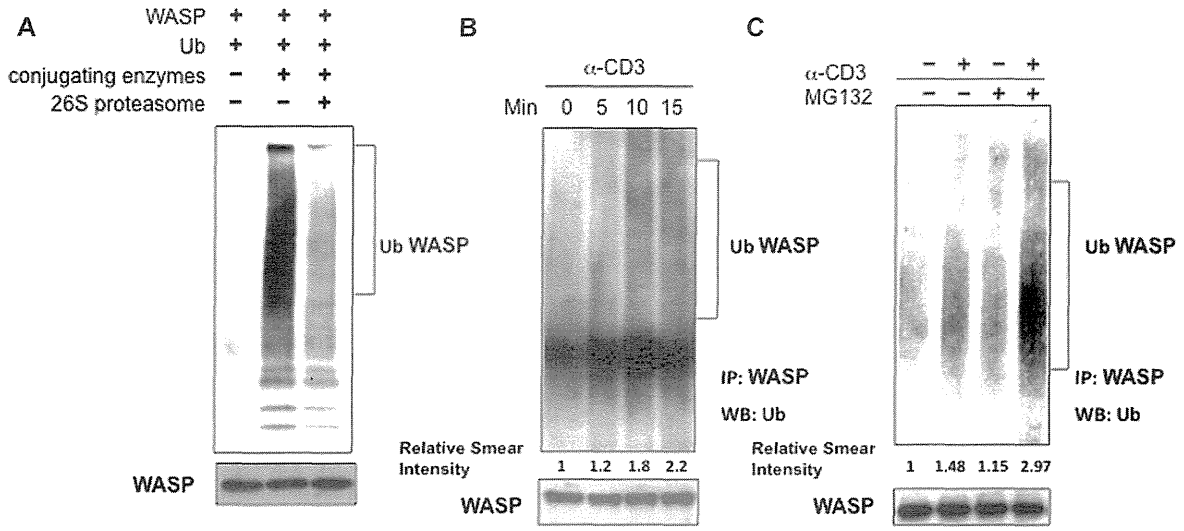

FIG 2. WASP is ubiquitinated and degraded by the 26S proteasome *in vitro* and in anti-CD3–stimulated Jurkat cells. **A,** Ubiquitination of *in vitro* translated purified WASP by ubiquitin-conjugating enzymes and its degradation by the 26S proteasome. Reaction mixtures were probed with anti-ubiquitin. **B,** Generation of ubiquitinated WASP in Jurkat T cells after stimulation with anti-CD3 mAb. WASP immunoprecipitates were probed with anti-ubiquitin mAb. Polyubiquitinated WASP appears as a smear. **C,** Protection of ubiquitinated WASP from degradation by the proteasome inhibitor MG132 in anti-CD3–stimulated Jurkat T cells. Similar results were obtained in Fig 2, *A* to *C*, in 4 independent experiments. The relative smear intensity in Fig 2, *B* and *C*, represents the mean of 4 experiments. *IP*, Immunoprecipitate; *Ub*, ubiquitin; *WB*, Western blot.

investigated whether Cbl proteins and WASP form a complex. WASP immunoprecipitates from Jurkat cell lysates were probed for c-Cbl and Cbl-b. c-Cbl, but not Cbl-b, coprecipitated weakly with WASP in unstimulated Jurkat T cells. TCR ligation increased the association of c-Cbl with WASP. It also induced the association of Cbl-b with WASP at 10 and 15 minutes after stimulation (Fig 3, *A*).

To investigate whether Cbl proteins act as E3 ubiquitin ligases for WASP, we transiently transfected 293T cells with plasmids coding for WT WASP, HA-tagged ubiquitin, FLAG-tagged c-Cbl, or FLAG-tagged Cbl-b. WASP coprecipitated with both c-Cbl and Cbl-b and was polyubiquitinated significantly more when co-transfected with ubiquitin, c-Cbl, and Cbl-b than with ubiquitin and empty vector (Fig 3, *B*).

To examine the role of Cbl-b in WASP ubiquitination after TCR ligation, we used purified T cells from spleens of *Cbl-b*$^{-/-}$ mice. Ubiquitination of WASP after TCR ligation was reduced, although not completely abrogated, in T cells from *Cbl-b*$^{-/-}$ mice (Fig 3, *C*), suggesting that WASP is a substrate for Cbl-b in antigen-stimulated T cells. We could not examine the role of c-Cbl on WASP ubiquitination after TCR ligation because we had no access to T cells from *c-Cbl*$^{-/-}$ mice.

WASP degradation after TCR/CD3 ligation limits TCR/CD3-driven F-actin assembly in T cells

WASP is important for F-actin assembly in T cells.[10] We examined whether WASP degradation after TCR/CD3 ligation regulates TCR/CD3-driven F-actin assembly. Purified T cells from WT and WASP-deficient mice were incubated for 6 hours with calpeptin or left untreated, washed and stimulated with anti-CD3 mAb, and cross-linked with a secondary antibody. The cells were then fixed, permeabilized, stained for F-actin with fluorescein isothiocyanate–conjugated phalloidin, and analyzed by means of flow cytometry. As previously reported, WASP-deficient T cells had a lower F-actin content than WT T cells.[16] TCR/CD3 ligation caused a parallel increase in F-actin levels in both WT and WASP-deficient T cells, which peaked at 5 minutes after stimulation and returned almost to baseline 10 minutes after stimulation. Pretreatment with calpeptin had no effect on F-actin content of the T cells at baseline or at 2 and 5 minutes after stimulation; however, it significantly increased the F-actin content of WT T cells at 10 minutes after anti-CD3 stimulation, maintaining it at almost the peak level achieved at 5 minutes after stimulation. In contrast, pretreatment with calpeptin had no effect on the F-actin content of WASP-deficient T cells 10 minutes after anti-CD3 stimulation. These results suggest that calpain-mediated WASP degradation limits the duration of F-actin assembly after TCR/CD3 ligation.

We next examined whether ubiquitination, which targets WASP for proteosomal degradation, regulates F-actin assembly after TCR/CD3 ligation. Because Cbl-b participates in WASP ubiquitination, we examined F-actin assembly in T cells deficient in Cbl-b. Baseline F-actin content and TCR-driven F-actin assembly were both significantly increased in T cells from c-Cbl-deficient mice compared with T cells from WT control animals (Fig 4, *B*). These results suggest that WASP degradation by ubiquitination regulates baseline and TCR-driven F-actin assembly.

DISCUSSION

Our results demonstrate that TCR ligation triggers the degradation of WASP by calpain-mediated cleavage and Cbl-mediated ubiquitination and subsequent proteasomal degradation. We present evidence that WASP degradation provides a mechanism for limiting the duration of TCR-driven assembly of F-actin.

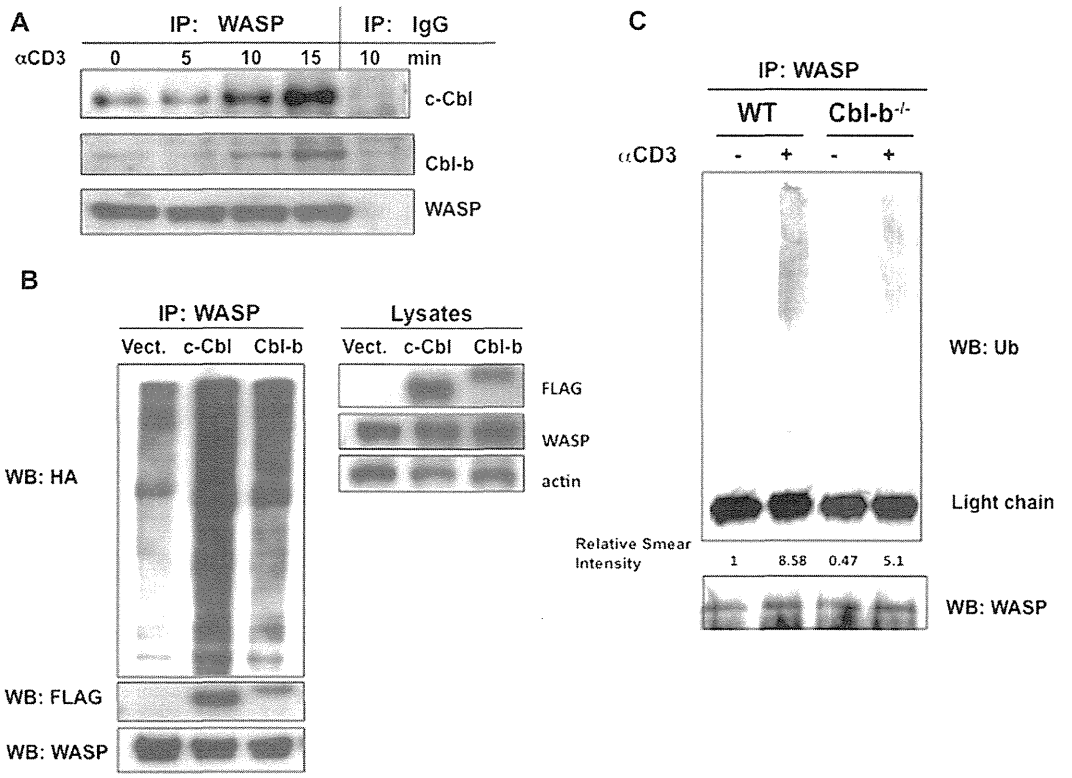

FIG 3. Cbl family E3 ubiquitin ligases associate with and ubiquitinate WASP after TCR ligation. **A,** Western blot analysis of WASP immunoprecipitates from anti-CD3–stimulated Jurkat T cells for c-Cbl and Cbl-b. IgG control antibody precipitates were prepared 10 minutes after anti-CD3 stimulation and used as controls. **B,** Ubiquitination of WASP in 293T cells transfected with WT WASP and HA-tagged ubiquitin plus either FLAG vector alone *(Vect.)*, FLAG-tagged c-Cbl, or FLAG-tagged Cbl-b. In the *left panel* WASP immunoprecipitates were probed for HA, FLAG, and WASP. In the *right panel* total lysates were probed for FLAG–c-Cbl or FLAG–Cbl-b, WASP, and actin. **C,** WASP ubiquitination after TCR ligation in T cells from *Cbl-b*$^{-/-}$ mice and WT control animals. WASP immunoprecipitates were probed for ubiquitin. Similar results were obtained in Fig 3, *A* to *C*, in 4 independent experiments. The relative smear intensity in Fig 3, *C*, represents the mean of 4 experiments. *IP*, Immunoprecipitate; *Ub*, ubiquitin; *WB*, Western blot.

TCR/CD3 ligation resulted in the degradation of a small fraction of WASP through calpain-mediated cleavage and the ubiquitin proteasome pathway. We estimated that approximately 5% of WASP is degraded after TCR/CD3 ligation. This is possibly an underestimate because the truncated 55-kDa WASP might be less stable than intact WASP. We could not detect a decrease in the levels of intact WASP in anti-CD3–activated T cells, probably because Western blotting is not sensitive enough to detect a small decrease in protein levels. We were unable to detect the cleaved, C-terminal, approximately 10-kDa fragment using an antibody to the C-terminus of WASP. This is most likely because such a small cleaved fragment would be rapidly degraded in the cell. Normally, WASP is protected from degradation by its partner, WIP.[16] The conformational changes in WASP induced by TCR signaling, which involve a change from an inactive to an active form capable of activating the Arp2/3 complex and F-actin polymerization, possibly increases the susceptibility of WASP to calpain cleavage and to ubiquitination and proteasomal degradation. The observation that WASP is degraded by calpain after TCR ligation is consistent with previous observations that WASP can be degraded in platelet lysates by calpain[29] and that *in vitro* translated WASP is a substrate for calpain I and II.[16] The increase in intracellular Ca^{++} concentration that follows TCR ligation could be the trigger for the Ca^{++}-dependent activation of calpain in anti-CD3–stimulated T cells.

Both c-Cbl and Cbl-b associated with WASP when overexpressed in 293T cells and acted as E3 ubiquitin ligases for WASP ubiquitination *in vitro*. More importantly, WASP ubiquitination after TCR ligation was impaired in Cbl-b-deficient T cells, implicating at least Cbl-b in WASP ubiquitination in T cells. Cbl family proteins act as negative regulators of TCR signaling by virtue of their ability to ubiquitinate LCK and ZAP-70,[33] which are upstream of WASP. Thus Cbl family members might regulate WASP activity indirectly by dampening TCR signaling upstream of WASP, as well as directly by ubiquitinating WASP and targeting it for degradation. Evidence has been presented that the activated WASP phosphorylated at Y291 is a target for ubiquitination.[34] We have also found that inhibition of the proteasome by MG132 increases the amount of tyrosine-phosphorylated WASP in anti-CD3–stimulated cells (see Fig E1 in this article's Online Repository at www.jacionline.org). This observation lends further support to the notion that activated WASP molecules are targets for degradation after TCR ligation.

It is not clear whether the interaction between WASP and c-Cbl and Cbl-b is direct or mediated by other proteins. It has been reported that c-Cbl associates with multiple proteins, which

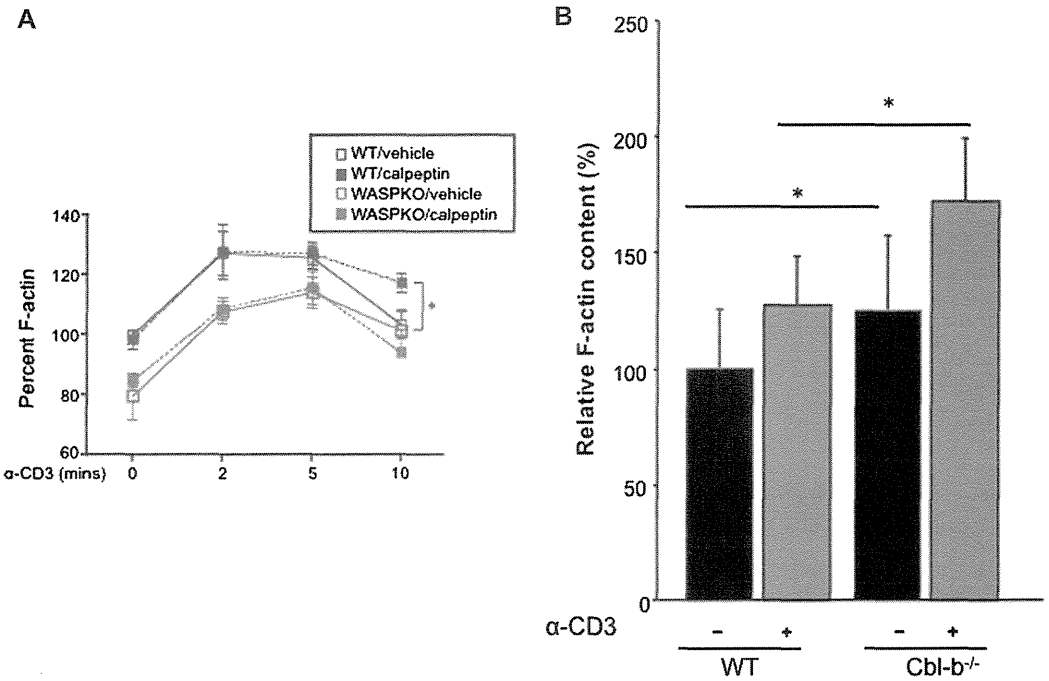

FIG 4. Effect of calpain inhibition and loss of Cbl on F-actin assembly in T cells. **A,** Effect of pretreatment of T cells from WT and WASP knockout mice with calpeptin on TCR-driven assembly of F-actin. Pretreatment with the vehicle dimethyl sulfoxide was used as a control. **B,** TCR-driven assembly of F-actin in T cells from *Cbl-b*$^{-/-}$ mice and WT control animals. T cells were stimulated with anti-CD3 for 10 minutes. Results are expressed as a percentage of the baseline F-actin content in unstimulated WT T cells and represent the means ± SDs of 3 independent experiments. **P* < .01.

include tyrosine phosphorylated ZAP-70,[35] the adaptor proteins Nck[36] and Grb2[37] through their SH3 domains, CrkL through its SH2 domain,[38] Src tyrosine kinases through their SH3 domains,[39,40] and Vav and the p85 regulatory subunit of phosphatidylinositol-3-OH kinase through their SH2 domains.[41,42] Because these proteins are also reported to associate with WASP, its partner WIP, or both,[17,43] an indirect association of Cbl with WASP cannot be ruled out. Alternatively, c-Cbl and Cbl-b could directly interact with an activated form of WASP, such as tyrosine-phosphorylated WASP. Indeed, while this manuscript was in preparation, it was shown that WASP phosphorylation at tyrosine 291 after TCR activation results in recruitment of Cbl-b.[34]

Our data suggest that the degraded fraction of WASP includes activated WASP. This is supported by the observation that calpain inhibition and lack of the WASP-ubiquitinating E3 ligase Cbl-b resulted in more sustained F-actin assembly in WT T cells after TCR/CD3 ligation. The small fraction of WASP that is cleaved after TCR ligation could be important for F-actin polymerization because of its location close to the TCR. Indeed, we have shown previously that a fraction of WASP translocates together with a fraction of the TCR/CD3 complex to lipid rafts.[17] It is also well known that a fraction of WASP colocalizes with TCR molecules in the immune synapse (IS).[17,44,45] Cbl family molecules, which are also recruited to the IS, where they are activated by LCK and ZAP-70,[46,47] could ubiquitinate WASP molecules recruited to the IS, targeting them for degradation. The IS is a dynamic structure that constantly undergoes protein kinase Cθ–dependent dissolution and WASP/F-actin–dependent reformation of its peripheral supramolecular activation complex.[45] Protein kinase Cθ–dependent dissolution breaks the symmetry of the IS and allows T-cell motility. WASP/F-actin–dependent reformation of the IS is important for the sustained signaling that is necessary for IL-2 production. We speculate that cycles of TCR-triggered recruitment and activation of WASP in the IS followed by local degradation of the activated WASP might be important for IS dynamics and T-cell function.

The observation that baseline F-actin content was increased in *Cbl-b*$^{-/-}$ T cells, but not in calpeptin-treated T cells, suggests that under steady-state conditions, Cbl ubiquitination and proteasome degradation, but not calpain, degrade WASP molecules in activated in T cells. The observation that calpain inhibition had no effect on F-actin assembly in WASP-deficient T cells indicates that calpain regulates F-actin assembly by targeting WASP for degradation. These results strongly suggest that degradation of activated WASP by calpain and by the ubiquitin/proteasome pathway provide an important homeostatic mechanism for terminating signaling to the cytoskeleton after TCR ligation. Furthermore, WASP mutants that are resistant to ubiquitination are associated with enhanced T-cell activation, supporting the notion that WASP degradation limits TCR activation.[34]

Protein cleavage is used by prokaryotes and eukaryotes to activate or terminate signaling. Well-documented examples include the coagulation cascade, the complement activation cascade, degradation of the nuclear factor κB inhibitor IκBα, TNF receptor–associated factor 3, Argonaute, and voltage-gated calcium-channel proteins.[48-53] Degradation of activated WASP might regulate receptor signaling to the cytoskeleton not only in T cells but also in other hematopoietic cells. Such a control mechanism would avoid the potential pathology observed in patients with mutations that cause sustained WASP activation and manifest as X-linked neutropenia.

We thank K. A. Siminovitch, H. Gu, N. Ishii, and Y. Tanaka for reagents and mice.

Key message

- **TCR signaling causes WASP to be degraded by calpain and by Cbl-family members through ubiquitination and destruction by the proteasome, limiting TCR-driven assembly of F-actin.**

REFERENCES

1. Ochs HD, Rosen FS. The Wiskott-Aldrich syndrome. 2nd ed. New York: Oxford University Press; 2006.
2. Derry JMJ, Ochs HD, Francke U. Isolation of a novel gene mutated in Wiskott-Aldrich syndrome. Cell 1994;78:635-44.
3. Kwan SP, Hagemann TL, Radtke BE, Blaese RM, Rosen FS. Identification of mutations in the Wiskott-Aldrich syndrome gene and characterization of a polymorphic dinucleotide repeat at DXS6940, adjacent to the disease gene. Proc Natl Acad Sci U S A 1995;92:4706-10.
4. Anton IM, Jones GE, Wandosell F, Geha R, Ramesh N. WASP-interacting protein (WIP): working in polymerisation and much more. Trends Cell Biol 2007;17:555-62.
5. Higgs HN, Pollard TD. Activation by Cdc42 and PIP2 of Wiskott-Aldrich syndrome protein (WASp) stimulates actin nucleation by Arp2/3 complex. J Cell Biol 2000;150:1311-20.
6. Ramesh N, Anton IM, Hartwig JH, Geha RS. WIP, a protein associated with Wiskott-Aldrich syndrome protein, induces actin polymerization and redistribution in lymphoid cells. Proc Natl Acad Sci U S A 1997;94:14671-6.
7. Badour K, Zhang J, Siminovitch KA. Involvement of the Wiskott-Aldrich syndrome protein and other actin regulatory adaptors in T cell activation. Semin Immunol 2004;16:395-407.
8. Huang Y, Burkhardt JK. T-cell-receptor-dependent actin regulatory mechanisms. J Cell Sci 2007;120:723-30.
9. Thrasher AJ. WASp in immune-system organization and function. Nat Rev Immunol 2002;2:635-46.
10. Gallego MD, Santamaria M, Pena J, Molina IJ. Defective actin reorganization and polymerization of Wiskott-Aldrich T cells in response to CD3-mediated stimulation. Blood 1997;90:3089-97.
11. Snapper SB, Rosen FS, Mizoguchi E, Cohen P, Khan W, Liu C-H, et al. Wiskott-Aldrich Syndrome protein-deficient mice reveal a role for WASP in T but not B cell activation. Immunity 1998;9:81-91.
12. Zhang J, Shehabeldin A, da Cruz LA, Butler J, Somani AK, McGavin M, et al. Antigen receptor-induced activation and cytoskeletal rearrangement are impaired in Wiskott-Aldrich syndrome protein-deficient lymphocytes. J Exp Med 1999;190:1329-42.
13. Cory GO, Garg R, Cramer R, Ridley AJ. Phosphorylation of tyrosine 291 enhances the ability of WASp to stimulate actin polymerization and filopodium formation. J Biol Chem 2002;277:45115-21.
14. Rohatgi R, Nollau P, Ho HY, Kirschner MW, Mayer BJ. Nck and phosphatidylinositol 4,5-bisphosphate synergistically activate actin polymerization through the N-WASP-Arp2/3 pathway. J Biol Chem 2001;276:26448-52.
15. Torres E, Rosen MK. Contingent phosphorylation/dephosphorylation provides a mechanism of molecular memory in WASP. Mol Cell 2003;11:1215-27.
16. de la Fuente MA, Sasahara Y, Calamito M, Anton IM, Elkhal A, Gallego MD, et al. WIP is a chaperone for Wiskott-Aldrich syndrome protein (WASP). Proc Natl Acad Sci U S A 2007;104:926-31.
17. Sasahara Y, Rachid R, Byrne MJ, de la Fuente MA, Abraham RT, Ramesh N, et al. Mechanism of recruitment of WASP to the immunological synapse and of its activation following TCR ligation. Mol Cell 2002;10:1269-81.
18. Lanzi G, Moratto D, Vairo D, Masneri S, Delmonte O, Paganini T, et al. A novel primary human immunodeficiency due to deficiency in the WASP-interacting protein WIP. J Exp Med 2012;209:29-34.
19. Moratto D, Giliani S, Notarangelo LD, Mazza C, Mazzolari E, Notarangelo LD. The Wiskott-Aldrich syndrome: from genotype-phenotype correlation to treatment. Expert Rev Clin Immunol 2007;3:813-24.
20. Ochs HD, Notarangelo LD. Structure and function of the Wiskott-Aldrich syndrome protein. Curr Opin Hematol 2005;12:284-91.
21. Massaad MJ, Ramesh N, Le Bras S, Giliani S, Notarangelo LD, Al-Herz W, et al. A peptide derived from the Wiskott-Aldrich syndrome (WAS) protein-interacting protein (WIP) restores WAS protein level and actin cytoskeleton reorganization in lymphocytes from patients with WAS mutations that disrupt WIP binding. J Allergy Clin Immunol 2011;127:998-1005, e1-2.
22. Devriendt K, Kim AS, Mathijs G, Frints SG, Schwartz M, Van Den Oord JJ, et al. Constitutively activating mutation in WASP causes X-linked severe congenital neutropenia. Nat Genet 2001;27:313-7.
23. Ochs HD. Mutations of the Wiskott-Aldrich syndrome protein affect protein expression and dictate the clinical phenotypes. Immunol Res 2009;44:84-8.
24. Beel K, Cotter MM, Blatny J, Bond J, Lucas G, Green F, et al. A large kindred with X-linked neutropenia with an I294T mutation of the Wiskott-Aldrich syndrome gene. Br J Haematol 2009;144:120-6.
25. Westerberg LS, Meelu P, Baptista M, Eston MA, Adamovich DA, Cotta-de-Almeida V, et al. Activating WASP mutations associated with X-linked neutropenia result in enhanced actin polymerization, altered cytoskeletal responses, and genomic instability in lymphocytes. J Exp Med 2010;207:1145-52.
26. Kawai S, Minegishi M, Ohashi Y, Sasahara Y, Kumaki S, Konno T, et al. Flow cytometric determination of intracytoplasmic Wiskott-Aldrich syndrome protein in peripheral blood lymphocyte subpopulations. J Immunol Methods 2002;260:195-205.
27. Tanaka Y, Tanaka N, Saeki Y, Tanaka K, Murakami M, Hirano T, et al. c-Cbl-dependent monoubiquitination and lysosomal degradation of gp130. Mol Cell Biol 2008;28:4805-18.
28. Du W, Kumaki S, Uchiyama T, Yachie A, Yeng Looi C, Kawai S, et al. A second-site mutation in the initiation codon of WAS (WASP) results in expansion of subsets of lymphocytes in an Wiskott-Aldrich syndrome patient. Hum Mutat 2006; 27:370-5.
29. Shcherbina A, Miki H, Kenney DM, Rosen FS, Remold-O'Donnell E. WASP and N-WASP in human platelets differ in sensitivity to protease calpain. Blood 2001; 98:2988-91.
30. Chou HC, Anton IM, Holt MR, Curcio C, Lanzardo S, Worth A, et al. WIP regulates the stability and localization of WASP to podosomes in migrating dendritic cells. Curr Biol 2006;16:2337-44.
31. Bachmaier K, Krawczyk C, Kozieradzki I, Kong YY, Sasaki T, Oliveira-dos-Santos A, et al. Negative regulation of lymphocyte activation and autoimmunity by the molecular adaptor Cbl-b. Nature 2000;403:211-6.
32. Paolino M, Penninger JM. Cbl-b in T-cell activation. Semin Immunopathol 2010; 32:137-48.
33. Krawczyk C, Penninger JM. Molecular controls of antigen receptor clustering and autoimmunity. Trends Cell Biol 2001;11:212-20.
34. Reicher B, Joseph N, David A, Pauker MH, Perl O, Barda-Saad M. Ubiquitylation-dependent negative regulation of WASp is essential for actin cytoskeleton dynamics. Mol Cell Biol 2012;32:3153-63.
35. Lupher ML Jr, Reedquist KA, Miyake S, Langdon WY, Band H. A novel phosphotyrosine-binding domain in the N-terminal transforming region of Cbl interacts directly and selectively with ZAP-70 in T cells. J Biol Chem 1996;271: 24063-8.
36. Miyoshi-Akiyama T, Aleman LM, Smith JM, Adler CE, Mayer BJ. Regulation of Cbl phosphorylation by the Abl tyrosine kinase and the Nck SH2/SH3 adaptor. Oncogene 2001;20:4058-69.
37. Donovan JA, Ota Y, Langdon WY, Samelson LE. Regulation of the association of p120cbl with Grb2 in Jurkat T cells. J Biol Chem 1996;271:26369-74.
38. Gesbert F, Garbay C, Bertoglio J. Interleukin-2 stimulation induces tyrosine phosphorylation of p120-Cbl and CrkL and formation of multimolecular signaling complexes in T lymphocytes and natural killer cells. J Biol Chem 1998;273: 3986-93.
39. Reedquist KA, Fukazawa T, Panchamoorthy G, Langdon WY, Shoelson SE, Druker BJ, et al. Stimulation through the T cell receptor induces Cbl association with Crk proteins and the guanine nucleotide exchange protein C3G. J Biol Chem 1996;271:8435-42.
40. Tanaka S, Neff L, Baron R, Levy JB. Tyrosine phosphorylation and translocation of the c-cbl protein after activation of tyrosine kinase signaling pathways. J Biol Chem 1995;270:14347-51.
41. Jain SK, Langdon WY, Varticovski L. Tyrosine phosphorylation of p120cbl in BCR/abl transformed hematopoietic cells mediates enhanced association with phosphatidylinositol 3-kinase. Oncogene 1997;14:2217-28.
42. Tartare-Deckert S, Monthouel MN, Charvet C, Foucault I, Van Obberghen E, Bernard A, et al. Vav2 activates c-fos serum response element and CD69 expression but negatively regulates nuclear factor of activated T cells and interleukin-2 gene activation in T lymphocyte. J Biol Chem 2001;276:20849-57.
43. Anton IM, Lu W, Mayer BJ, Ramesh N, Geha RS. The Wiskott-Aldrich syndrome protein-interacting protein (WIP) binds to the adaptor protein Nck. J Biol Chem 1998;273:20992-5.
44. Cannon JL, Labno CM, Bosco G, Seth A, McGavin MH, Siminovitch KA, et al. Wasp recruitment to the T cell:APC contact site occurs independently of Cdc42 activation. Immunity 2001;15:249-59.
45. Sims TN, Soos TJ, Xenias HS, Dubin-Thaler B, Hofman JM, Waite JC, et al. Opposing effects of PKCtheta and WASp on symmetry breaking and relocation of the immunological synapse. Cell 2007;129:773-85.

46. Elly C, Witte S, Zhang Z, Rosnet O, Lipkowitz S, Altman A, et al. Tyrosine phosphorylation and complex formation of Cbl-b upon T cell receptor stimulation. Oncogene 1999;18:1147-56.
47. Wiedemann A, Muller S, Favier B, Penna D, Guiraud M, Delmas C, et al. T-cell activation is accompanied by an ubiquitination process occurring at the immunological synapse. Immunol Lett 2005;98:57-61.
48. Schenone M, Furie BC, Furie B. The blood coagulation cascade. Curr Opin Hematol 2004;11:272-7.
49. Forneris F, Wu J, Gros P. The modular serine proteases of the complement cascade. Curr Opin Struct Biol 2012;22:333-41.
50. Baud V, Derudder E. Control of NF-kappaB activity by proteolysis. Curr Top Microbiol Immunol 2011;349:97-114.
51. Bronevetsky Y, Villarino AV, Eisley CJ, Barbeau R, Barczak AJ, Heinz GA, et al. T cell activation induces proteasomal degradation of Argonaute and rapid remodeling of the microRNA repertoire. J Exp Med 2013;210:417-32.
52. Razani B, Reichardt AD, Cheng G. Non-canonical NF-kappaB signaling activation and regulation: principles and perspectives. Immunol Rev 2011;244:44-54.
53. De Jongh KS, Colvin AA, Wang KK, Catterall WA. Differential proteolysis of the full-length form of the L-type calcium channel alpha 1 subunit by calpain. J Neurochem 1994;63:1558-64.

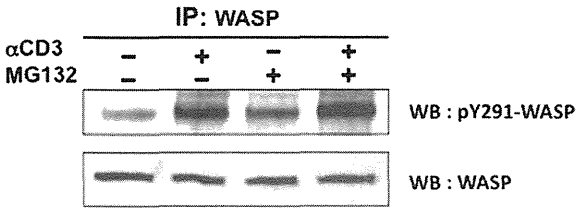

FIG E1. Tyrosine-phosphorylated WASP generated after TCR ligation is a target for proteasomal degradation. Effect of pretreatment of MG132 on the amount of tyrosine-phosphorylated WASP in anti-CD3–stimulated Jurkat T cells is shown. WASP immunoprecipitates were probed with anti-pY291-WASP antibody (Abcam). Similar results were obtained in 3 experiments. *IP*, Immunoprecipitate; *WB*, Western blot.

PLOS ONE

Gene Therapy Model of X-linked Severe Combined Immunodeficiency Using a Modified Foamy Virus Vector

Satoshi Horino[1,2], Toru Uchiyama[2], Takanori So[1], Hiroyuki Nagashima[1], Shu-lan Sun[1], Miki Sato[2], Atsuko Asao[1], Yoichi Haji[1], Yoji Sasahara[2], Fabio Candotti[3], Shigeru Tsuchiya[2], Shigeo Kure[2], Kazuo Sugamura[4], Naoto Ishii[1]*

1 Department of Microbiology and Immunology, Tohoku University Graduate School of Medicine, Sendai, Japan, **2** Department of Pediatrics, Tohoku University Graduate School of Medicine, Sendai, Japan, **3** Genetics and Molecular Biology Branch, National Human Genome Research Institute, National Institutes of Health, Bethesda, Maryland, United States of America, **4** Miyagi Cancer Center, Natori, Japan

Abstract

X-linked severe combined immunodeficiency (SCID-X1) is an inherited genetic immunodeficiency associated with mutations in the common cytokine receptor γ chain (γc) gene, and characterized by a complete defect of T and natural killer (NK) cells. Gene therapy for SCID-X1 using conventional retroviral (RV) vectors carrying the γc gene results in the successful reconstitution of T cell immunity. However, the high incidence of vector-mediated T cell leukemia, caused by vector insertion near or within cancer-related genes has been a serious problem. In this study, we established a gene therapy model of mouse SCID-X1 using a modified foamy virus (FV) vector expressing human γc. Analysis of vector integration in a human T cell line demonstrated that the FV vector integration sites were significantly less likely to be located within or near transcriptional start sites than RV vector integration sites. To evaluate the therapeutic efficacy, bone marrow cells from γc-knockout (γc-KO) mice were infected with the FV vector and transplanted into γc-KO mice. Transplantation of the FV-treated cells resulted in the successful reconstitution of functionally active T and B cells. These data suggest that FV vectors can be effective and may be safer than conventional RV vectors for gene therapy for SCID-X1.

Citation: Horino S, Uchiyama T, So T, Nagashima H, Sun S-l, et al. (2013) Gene Therapy Model of X-linked Severe Combined Immunodeficiency Using a Modified Foamy Virus Vector. PLoS ONE 8(8): e71594. doi:10.1371/journal.pone.0071594

Editor: Lishomwa C. Ndhlovu, University of Hawaii, United States of America

Received June 3, 2013; **Accepted** July 8, 2013; **Published** August 21, 2013

Funding: This study was supported in part by a grant-in-aid (#24659487 and #24390118) for scientific research on priority areas from the Ministry of Education, Science, Sports and Culture of Japan, a grant-in-aid for scientific research on priority areas from the Japan Society for the Promotion of Science, and grants (#111020001010004100) from the Japan Science and Technology Agency. The funders had no role in study design, data collection and analysis, decision to publish, or preparation of the manuscript. No additional external funding was received for this study.

Competing Interests: The authors have declared that no competing interests exist.

* E-mail: ishiin@med.tohoku.ac.jp

Introduction

X-linked severe combined immunodeficiency (SCID-X1) is a life-threatening immunodeficiency disorder, characterized by defective T and natural killer (NK) cell production and the development of functionally impaired B cells that lack the capacity to produce immunoglobulins. These defects result in a profound reduction in the development of both cellular and humoral immunity. SCID-X1 is caused by inactivating mutations in the gene encoding the cytokine receptor γ chain (γc), a common subunit of the receptors for interleukin (IL)-2, IL-4, IL-7, IL-9, IL-15, and IL-21 [1]. Bone marrow transplantation (BMT) from human leukocyte antigen (HLA)-identical siblings can cure the disease with a success rate of approximately 90%. However, BMT from non-HLA-identical donors results in lower survival rates due to a high risk for complications such as graft-versus-host disease, graft rejection, and incomplete T cell engraftment [2,3]. Consequently, gene therapy approaches have been developed as an alternative treatment option for those patients lacking appropriate donors.

The first gene therapy clinical trial for SCID-X1 was carried out by a French group in 1999 [4,5]. In that study, a conventional retroviral (RV) vector expressing γc was used, and resulted in the reconstitution of T and NK cell populations, and the recovery of humoral immunity. However, over time, acute T cell leukemia developed in 5 of the 20 patients receiving the therapy. The leukemia cells of these patients showed aberrant and high expressions of proto-oncogenes such as *LMO2*, which were caused by RV insertions within or near these loci [4,5]. To reduce the risk of vector-mediated insertional mutagenesis, various types of new vectors have since been developed [6,7].

Foamy virus (FV) is a non-pathogenic retrovirus belonging to the spumavirus genus and has unique biological characteristics, such as a wide host range (including humans), and wide tissue tropism [8,9]. Refined FV vectors that have large packaging capacities and are able to transduce murine and human hematopoietic stem cells (HSCs) have been reported [10–12]. In addition, FV vectors are reported to have a reduced tendency to integrate within or adjacent to the coding regions of genes compared to RV vectors. Due to these advantages, FV vectors have recently been used to correct genetic deficiencies in hematopoietic stem cells (HSCs) in several mouse models; these diseases include Wiskott–Aldrich syndrome (WAS) [13], leukocyte adhesion deficiency [14], Fanconi anemia [15], β-thalassemia [16], and X-linked chronic granulomatous disease [17].

In the present study, we evaluated the rate of insertional mutagenesis by a γc-FV vector compared to that of an RV vector in human T cells, and demonstrated the effectiveness of the γc-FV vector in a murine gene therapy model of SCID-X1.

Methods

All procedures were performed according to the protocols approved by the Institutional Committee for Use and Care of Laboratory Animals of Tohoku University, which was granted by Tohoku University Ethics Review Board (No. 2010MA165) and the Guide for Care and Use of Laboratory Animals published by the U.S. National Institutes of Health (NIH publication 85–23, revised 1996).

FV vector construction and production

FV vector plasmids were constructed as previously described [13,18,19]. In brief, a 631-bp *BspE*I and *Tth111*I restriction fragment from the ubiquitously acting chromatin-opening element promoter from the human HNRPA2B1-CBX3 locus (UCOE631) was isolated and inserted into the pΔΦ vector plasmid together with either the human γc (*IL2RG*) or enhanced green fluorescent protein (EGFP) complementary DNA (cDNA) to generate FV-IL2RG and FV-EGFP (Fig. 1A).

FV particles were produced by transfecting 293T cells with the resultant gene transfer vector plasmids and three helper plasmids (pCiGS, pCiPS, and pCiES) using FuGENE HD (Roche Applied Science), as previously described [13]. Culture supernatants were harvested after 48 hours and concentrated by ultracentrifugation.

A γc RV vector was constructed by inserting the human γc cDNA into the multi-cloning site of pMX-IRES-EGFP. Retroviral particles were produced by transfecting into amphotropic retrovirus packaging cells (PLAT-A cells) with pMx-IL2RG-IRES-EGFP using FuGENE HD. Culture supernatants containing the RV vector particles were harvested after 48 hours.

Cell lines

A human T cell line, ED40515(−) [20], which lacks γc expression, and an ED40515(−)-derived transfectant with a γc gene, EDγ, were described previously [21,22]. These cell lines were cultured in RPMI1640 medium supplemented with 10% FCS.

Mice

The γc-KO mice were previously reported [23]. γc-KO mice on a NOD/scid background [24] were obtained from the Central Institute for Experimental Animals (CIEA, Kawasaki, Japan). They were housed under specific pathogen-free conditions in individually ventilated cages and supplied with sterile food, water, and bedding. All procedures were performed according to protocols approved by the Institutional Committee for the Use and Care of Laboratory Animals of Tohoku University (2011MA139).

Vector transduction and BMT

Lineage marker depleted (Lin^-) cells were purified from the bone marrow cells of male γc-KO mice using magnetic cell sorting. The purified cells were exposed to FV vectors in StemSpan medium (StemCell Technologies Japan, Tokyo) supplemented with stem cell factor (50 ng/ml), IL-3 (5 ng/ml), Flt-3 ligand (5 ng/ml), and IL-6 (10 ng/ml) (all from Wako Pure Chemical Industries, Tokyo, Japan) on CH-296 (Retronectin; Takara Shuzo, Otsu, Japan)-coated plates for 16 hours. The transduced cells ($1–3\times10^6$) were then transplanted intravenously into 120 rad-irradiated female γc-KO mice on a NOD/scid background of 6–8 weeks of age. Eight to 12 weeks after BMT, and the peripheral blood cells and splenocytes were analyzed.

The ED40515 cell lines were similarly transduced with FV or RV vectors, except that cytokines were not added.

Immunofluorescence staining

For fluorescence-activated cell sorting (FACS) analysis, peripheral blood cells and splenocytes were collected from the mice. After removing erythrocytes with a lysing buffer, the cells were stained with anti-CD3-allophycocyanin (APC), anti-CD4-APC, anti-CD8-phycoerythrin (PE), anti-NK1.1-PE, anti-B220-APC, and/or anti-IgM-PE monoclonal antibodies (mAbs). Stained cells

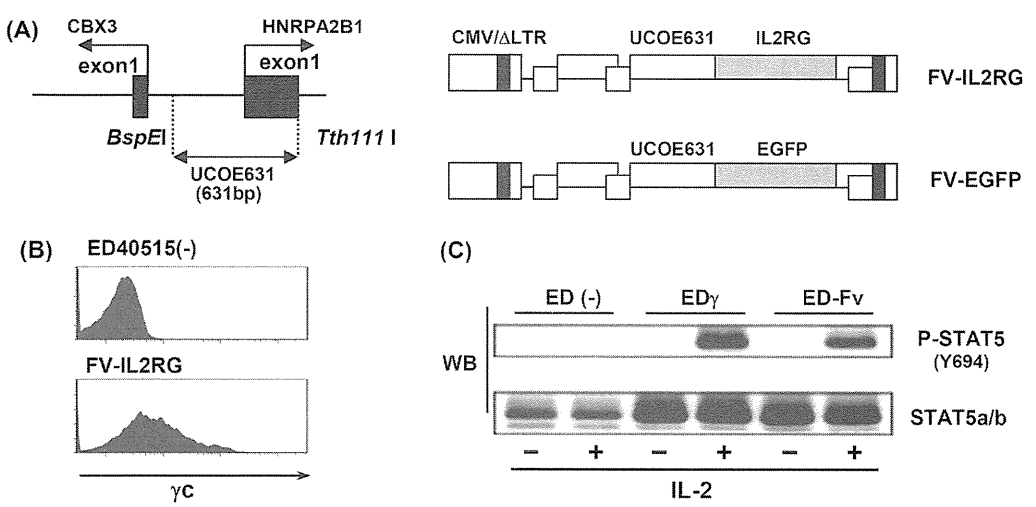

Figure 1. Structure and *in vitro* analysis of foamy virus vectors. (**A**) Structure of the foamy virus vectors. The UCOE631 promoter sequence from the human HNRPA2B1-CBX3 locus and transgenes were inserted into the FV vector. (**B**) Cell-surface expression of γc on ED40515(−) cells transduced with the FV-IL2RG vector. (**C**) STAT5 phosphorylation upon IL-2 stimulation. ED40515(−) cells, an ED40515(−)-derived transfectant with a γc gene, EDγ cells, and ED40515(−) cells transduced with the indicated vectors were stimulated with IL-2 for 30 min, and STAT5 phosphorylation in each cell line was detected by a STAT5 phosphospecific mAb.
doi:10.1371/journal.pone.0071594.g001

were analyzed with a FACS CantoII analyzer using the FACS Diva software (BD Biosciences, San Jose, CA).

Phosphorylated STAT5 detection

The IL-2-induced phosphorylation of STAT5 was detected by Western blotting as previously described [22]. In brief, cells were stimulated with 100 ng/ml IL-2 for 30 min at 37°C, collected, and lysed with a lysis buffer (20 mM Tris-HCl (pH 7.4), 150 mM NaCl, 2 mM EDTA, 1% NP-40, 50 mM NaF, 1 mM Na_3VO_4, and Protease Inhibitor Cocktail (Sigma-Aldrich Japan, Tokyo)). The protein lysates were separated by electrophoresis, transferred onto a polyvinylidene fluoride membrane, and blotted with STAT5 phosphospecific (pY694) antibodies (Cell Signaling Technology, Japan). Bound primary Abs were detected by a horseradish peroxidase-conjugated anti-rabbit IgG Ab followed by an enhanced chemiluminescence (ECL) detection reagent.

T cell proliferation and cytokine production

Spleen cells (1×10^5 cells/well) were stimulated with plate-coated anti-CD3 mAb (clone 2C11; 0.5 or 10 μg/ml) and/or 100 ng/ml recombinant human IL-2. T cell proliferation was measured after 48 hours by [^{3}H] thymidine incorporation and scintillation counting in triplicate. The stimulation index was calculated as the ratio of the incorporated radioactivity (cpm) of splenocytes from mice treated with FV-IL2RG-treated HSCs to that of splenocytes from mice treated with FV-EGFP-treated HSCs. IL-2 and IFN-γ production was assessed with an OptiEIA ELISA kit (BD Biosciences) after 24 hours and 72 hours, respectively, of stimulation, following the manufacturer's specifications.

Analysis of vector-insertion sites by ligation-mediated PCR

To determine the vector-integration sites, linker-mediated PCR was performed on genomic DNA isolated from γc-transduced ED40515(−) cells as previously described [13,25]. Briefly, the genomic DNA was digested with *Mse*I and *Pst*I, and the fragments were ligated to an MseI linker (5′-GTAATACGACTCACTA-TAGGGCTCCGCTTAAGGGACGAGGCGAATTCCCT-GAT-3′, 5′-PO4-TAGTCCCTTAAGCGGAG-NH2-3′). PCR was then performed with a linker-specific primer 5′-GTAATAC-GACTCACTATAGGGC-3′, and an FV long-terminal repeat-specific primer 5′-GTCTATGAGGAGCAGG AGTA-3′ or an RV long-terminal repeat-specific primer 5′-TAACCAAT-CAGTTCGCTTCTCGCTT-3′. A nested PCR was then performed using a linker-specific primer 5′-AGGGCTCCGCT-TAAGGGAC-3′, and an FV long-terminal repeat-specific primer 5′-CCTCCTTCCCTGTAATACTC-3′ or an RV long-terminal repeat-specific primer 5′-CTCAATAAAAGAGCCCA-CAACCCC-3′. The PCR products were subcloned into pCR2.1 using the TOPO cloning kit (Life Technologies Japan, Tokyo), and the vector/DNA junction sites were sequenced with an ABI 3100 Genetic Analyzer (Applied Biosystems). The recovered vector/DNA junctions were matched to the human genome using the BLAT software program and each insertion locus was identified. Since integration sites of conventional RV vectors are preferentially found within 15 kb of transcriptional start sites (TSS) [26,27], we calculated the percentages of all integration sites within 15 kb of TSS. The integration frequency was calculated as previously described [28]. In brief, FV vector integration sites were mapped relative to RefSeq gene transcription start sites, binned into different size sequence windows, and plotted as the percent of all integrations per kb. Genes within 30 kb of the integration sites were also compared to the list of annotated cancer genes in the Atlas of Genetics and Cytogenetics in the Oncology and Hematology database (http://atlasgeneticsoncology.org/).

Statistical analysis

Statistical analysis was performed using χ^2-test or Student's t-test. P-values <0.05 were considered significant.

Results

FV vector performance in human T cells

We constructed two FV vectors, FV-IL2RG and FV-EGFP, to express human γc and EGFP, respectively, both of which were driven by the ubiquitously acting chromatin-opening element promoter (Fig. 1A, and see Materials and Methods). This promoter consists of a methylation-free CpG island without classic enhancer activity. To evaluate the function of the FV-IL2RG vector-expressed γc chain, we infected ED40515(−), a human T cell line lacking γc [21,22], with the FV vectors. A flow cytometric analysis detected clear γc expression on the surface of the FV-IL2RG-treated cells (Fig. 1B). Western blot analysis showed the phosphorylation of Stat5 upon IL-2 stimulation, reflecting the activation of intracellular signaling through the vector-mediated γc (Fig. 1C), and indicating the expression of functional γc. These results indicated that FV vectors can effectively transfer and express the γc gene in human T cells.

Profile of provirus integration sites in human T cells

We identified 100 independent integration sites of the FV or RV provirus in ED40515(−) cells infected with each vector, using a standard linker-mediated PCR analysis. Fig. 2A shows that the frequency of integration sites located within gene transcriptional units was comparable between the FV (36%) and RV (42%) vectors. However, the FV integration sites showed a significantly lower likelihood (13%) of being located immediately up or downstream of transcriptional start sites than the RV integration sites (25%) (Fig. 2A). Furthermore, the FV integration sites in the human T cells showed only a modest preference for regions near transcriptional start sites compared to RV integration sites (Fig. 2B), consistent with the results of previous studies [13,25,29].

In addition, we examined the cancer-related genes located within 30 kb of the FV and RV integration sites because all the RV insertion sites in gene therapy-related leukemia were shown within gene or within 30 kb of TSS of LMO-2 or BMI1 [30]. One of the 100 FV integration sites was detected inside the cancer-related gene, TCF12, which is known as a negative regulator of cell proliferation, whereas three of the RV integration sites were detected within cancer-related genes, (Klf5, NUMB, and FHIT) all of which are known leukemia-related genes.

Collectively, these results suggest that FV vectors might have a lower risk of vector-mediated genotoxicity than conventional RV vectors.

In vivo assessment of T cell restoration after FV-mediated gene therapy

To evaluate the efficacy of FV vector-mediated γc expression *in vivo*, we performed BMT experiments. Bone marrow Lin$^-$ cells from γc-KO mice were transduced with FV-IL2RG or FV-EGFP vectors. The cellular transduction efficiency of both vectors was between 33 and 40%. The FV vector-infected cells were intravenously transplanted into γc-KO mice on a NOD/scid background. Since older γc-KO mice on a C57BL/6 background were found to contain CD3$^+$CD4$^+$ cells (data not shown), γc-KO

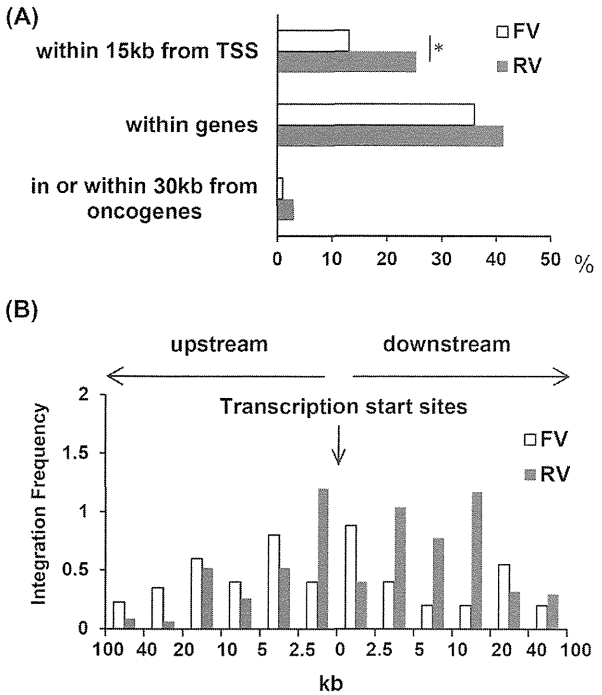

Figure 2. Profile of provirus integration in transduced cells. (**A**) Position of FV and RV integration sites. The percentage of all integration sites within 15 kb of transcriptional start sites, within genes that contain putative microRNA genes, and within 30 kb of oncogenes is shown for FV vector- or RV vector-treated cells. *$p<0.05$, χ^2-test. (**B**) A 100-kb window centered on TSS in the RefSeq database is shown. Relative frequencies of FV and RV vector integrations in each interval were calculated by dividing the percentage of integration b the indicated interval length.
doi:10.1371/journal.pone.0071594.g002

mice on a NOD/scid background were deemed a more suitable recipient for evaluating T cell reconstitution.

Eight weeks after transplantation, T cells emerged in the peripheral blood of the FV-IL2RG-treated group, and the clear expression of γc was confirmed on $CD8^+$ T cells (Fig. 3A). Gene therapy mice showed the recovery of CD4 and CD8 T cells as well as $B220^+$ IgM^+ B cells in spleen (in Figure 3B) although we could not detect NK cells. In addition, serum levels of IgM, IgG, and IgA were significantly elevated in FV-IL2RG-treated mice (Fig. 3C). These results indicate that HSCs transduced with FV-IL2RG have the potential for normal B and T cell differentiation.

We next investigated the functional capacity of the reconstituted T cells. Splenocytes from FV-IL2RG-treated mice showed proliferative responses following treatment with an anti-CD3 mAb, while those from the FV-EGFP-treated group did not (Fig. 4A). IL-2 stimulation induced proliferation through γc-transduced signals in T cells from FV-IL2RG-treated mice although stimulation with anti-CD3 mAb plus IL-2 did not enhance T cell proliferation compared to anti-CD3 mAb alone (Fig. 4A). The reconstituted T cells also produced IL-2 and IFN-γ upon stimulation with anti-CD3 mAb (Fig. 4B), indicating the functional restoration of T cells. Collectively, FV vector-mediated γc gene transfer was demonstrated to restore T and B cell differentiation and function *in vivo*.

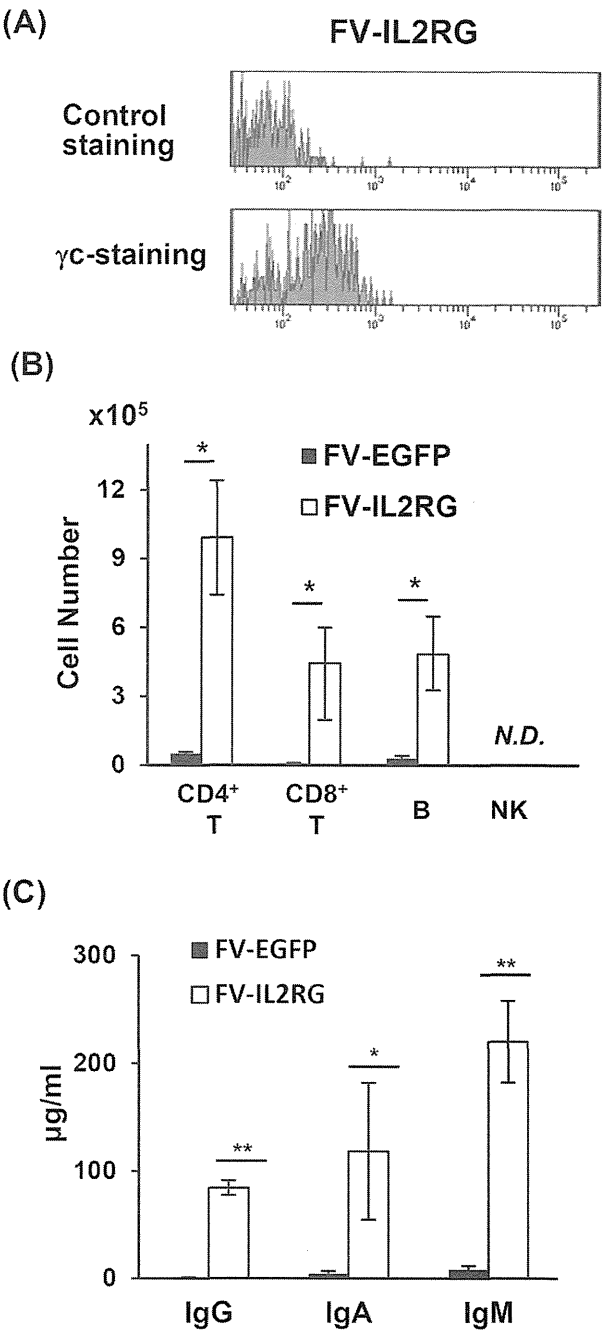

Figure 3. Reconstitution of T and B cells. (**A**) Cell-surface expression of γc on peripheral $CD8^+$ T cells in γc-KO mice treated with FV-IL2RG-treated HSCs. The upper and lower panels show isotype-control and γc-specific stainings, respectively. (**B**) The absolute numbers of $CD4^+$ T, $CD8^+$ T, $sIgM^+$ B, and NK cells in the spleen of γc-KO mice treated with FV-EGFP and FV-IL2RG (n = 4 in each group). *N.D.*, not detectable. (**C**) Serum IgM, IgG, and IgA in FV-IL2RG-treated mice. Serum levels of IgM, IgG, and IgA were measured by ELISA. Results shown are the mean ± SD of the stimulation index from 4 mice in each group. *$p<0.05$ and **$p<0.01$, Student t-test.
doi:10.1371/journal.pone.0071594.g003

Discussion

Vector-mediated insertional mutagenesis is a critical problem associated with conventional RV-mediated gene therapy treatments for SCID-X1. To address this issue, we developed a

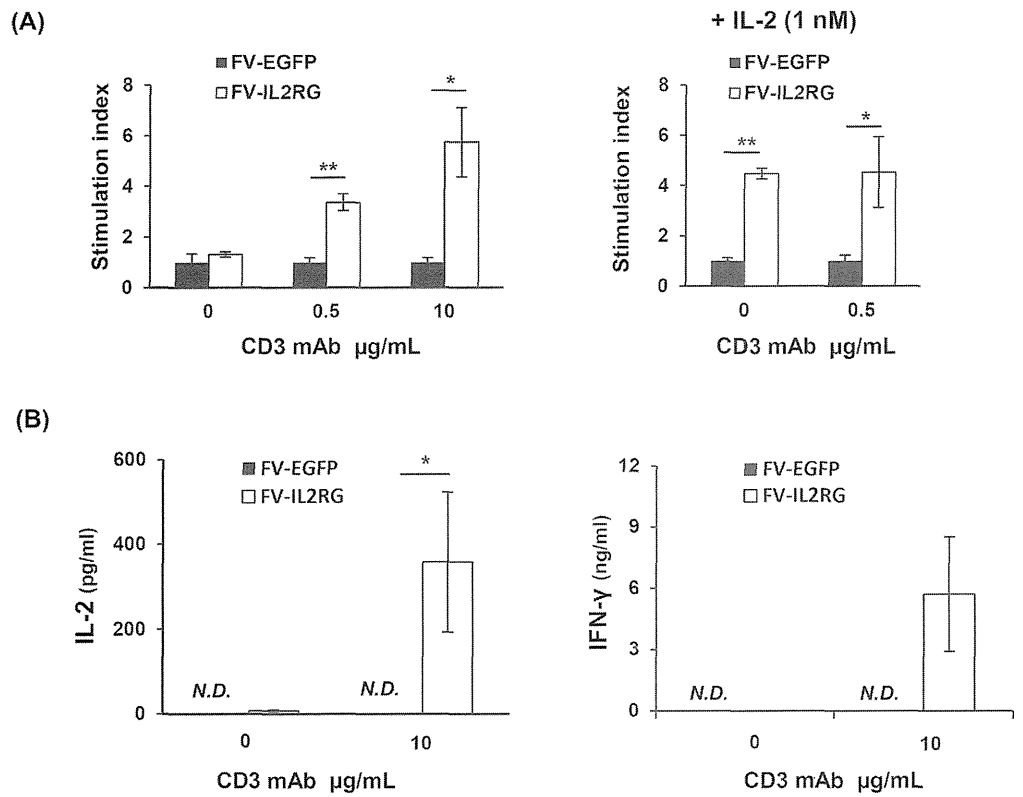

Figure 4. In vitro function of reconstituted T cells. (**A**) Splenocytes from recipient mice were stimulated with an anti-CD3 mAb at the indicated dose in the presence (right) or absence (left) of IL-2. Results shown are the mean ± SD of the stimulation index from 4 or 5 mice in each group. *p<0.05 and **p<0.01, Student t-test. (**B**) IL-2 and IFN-γ production by reconstituted T cells. Splenocytes from recipient mice were stimulated with an anti-CD3 mAb at the indicated dose. Culture supernatants were collected 24 and 72 hours after stimulation. Concentration of each cytokine in the supernatant was measured by ELISA. Results shown are the mean ± SD from 4 mice in each group. *p<0.05, Student t-test. *N.D.*, not detectable.
doi:10.1371/journal.pone.0071594.g004

modified FV vector carrying the human γc gene, and evaluated the vector-mediated insertional mutagenesis as well as the *in vivo* T, B, and NK cell reconstitution. Our findings demonstrated that the integration sites of the FV vector were significantly less likely to be located within or near transcriptional start sites compared to those of a conventional RV vector, suggesting that the FV vector had a lower risk for insertion-mediated genotoxicity. We also showed the successful reconstitution of functionally active T and B cells after the transplantation of HSCs containing a γc-FV vector into γc-KO recipient mice. This is the first reported use of an FV vector in a gene therapy mouse model of SCID-X1.

Previous studies showed that the use of classical RV vector for SCID-X1 gene therapy resulted in the development of leukemia in a number of patients [4,5]. The leukemogenesis associated with these vectors is likely to be due to inappropriate vector insertion in or near proto-oncogenes. Consistent with previous reports that FV vectors have a more random genomic integration pattern than RV vectors [28], our data indicated that the FV vector integration sites were less likely to be near transcription start sites than those of RV vectors (Fig. 2A, 2B). In addition, three integration sites of the RV vector were found within cancer-related genes (Klf5, NUMB, and FHIT), all of which are associated with leukemogenesis or leukemia progression [31–33]. Although one FV vector integration site was found within a cancer-related gene, TCF12, no evidence showing a relationship between TCF12 and leukemogenesis has been reported. These results are consistent with the accepted theory that FV is non-pathogenic for humans [8,9], and support the notion that FV vectors may be safer than conventional RV vectors.

The main objective of SCID-X1 gene therapy is the robust reconstitution of T, B, and NK cells. However, in the present study, use of the FV-IL2RG vector failed to reconstitute the NK cell population when monitored up to 4 months after gene therapy. One possible explanation for this deficiency may be that the human γc gene is not entirely compatible with the mouse system. Consistent with our findings, impaired NK cell reconstitution in mouse SCID-X1 gene therapy using the human γc gene was previously reported [34]; however, gene therapies in mouse models with RV vectors carrying the mouse γc gene were shown to reconstitute NK cells within two months [35–37]. NK cell development requires IL-15, while the differentiation and survival of T and B cells require IL-7. Receptors for both cytokines contain the shared γc subunit [1]. Therefore, the human γc might function less effectively as a mouse IL-15 receptor subunit than as a mouse IL-7 receptor subunit. In addition, T cell responses to IL-2 might also be insufficient as additional stimulation of IL-2 did not increase the T cell response with anti-CD3 mAb alone. Namely, the chimeric IL-2 and IL-15 receptors consisting of mouse α and β chains in combination with human γc might not fully function as a physiological mouse IL-2 and IL-15 receptors, respectively. In any case, the use of human γc, rather than the FV vector, is the probable cause of the impaired NK cell reconstitution and possible insufficient T cell function in this study.

We recently reported the successful treatment of a WAS mouse model using gene therapy with an FV vector [13]. Similar to

SCID-X1, the gene therapy for WAS requires T cell proliferative and functional restoration. Our studies collectively support the potential for modified FV vector-mediated gene therapy for the successful treatment of T cell immunodeficiencies. Moreover, FV vectors have also been shown to be effective for the treatment of red blood cell and granulocyte disorders in mouse models [14–17]. Based on their broad host range and ability to efficiently transduce HSCs, FV vectors may be applicable in gene therapies for many different hematopoietic disorders.

Over the last decade, novel modifications of RV vectors have been developed to overcome the problems associated with SCID-X1 gene therapy. However, it is still controversial which vector is the most favorable for safety. FV vectors have the potential to increase the efficacy of HSC-based gene therapies and to reduce the risk of genotoxicity. Although further studies are necessary, our data support the potential clinical application of FV vectors in gene therapy for SCID-X1 in the future.

Acknowledgments

We sincerely thank Drs. David W. Russell (University of Washington) and Adrian J. Thrasher (University College of London) for sharing reagents. We also thank the Biomedical Research Core Animal Pathology Platform for the essential technical support of pathological analysis.

Author Contributions

Conceived and designed the experiments: NI TU. Performed the experiments: SH TS HN SLS MS AA YH. Analyzed the data: ST SK KS. Contributed reagents/materials/analysis tools: TU YS FC. Wrote the paper: NI SH TU.

References

1. Sugamura K, Asao H, Kondo M, Tanaka N, Ishii N, et al. (1996) The interleukin-2 receptor gamma chain: its role in the multiple cytokine receptor complexes and T cell development in XSCID. Annu Rev Immunol 14: 179–205.
2. Buckley RH, Schiff SE, Schiff RI, Markert L, Williams LW, et al. (1999) Hematopoietic stem-cell transplantation for the treatment of severe combined immunodeficiency. N Engl J Med 340: 508–516.
3. Haddad E, Landais P, Friedrich W, Gerritsen B, Cavazzana-Calvo M, et al. (1998) Long-term immune reconstitution and outcome after HLA-nonidentical T-cell-depleted bone marrow transplantation for severe combined immunodeficiency: a European retrospective study of 116 patients. Blood 91: 3646–3653.
4. Fischer A, Hacein-Bey-Abina S, Cavazzana-Calvo M (2010) 20 years of gene therapy for SCID. Nat Immunol 11: 457–460.
5. Cavazzana-Calvo M, Fischer A (2007) Gene therapy for severe combined immunodeficiency: are we there yet? J Clin Invest 117: 1456–1465.
6. Montini E, Cesana D, Schmidt M, Sanvito F, Bartholomae CC, et al. (2009) The genotoxic potential of retroviral vectors is strongly modulated by vector design and integration site selection in a mouse model of HSC gene therapy. J Clin Invest 119: 964–975.
7. Modlich U, Navarro S, Zychlinski D, Maetzig T, Knoess S, et al. (2009) Insertional transformation of hematopoietic cells by self-inactivating lentiviral and gammaretroviral vectors. Mol Ther 17: 1919–1928.
8. Russell DW, Miller AD (1996) Foamy virus vectors. J Virol 70: 217–222.
9. Stirnnagel K, Luftenegger D, Stange A, Swiersy A, Mullers E, et al. (2010) Analysis of prototype foamy virus particle-host cell interaction with autofluorescent retroviral particles. Retrovirology 7: 45.
10. Vassilopoulos G, Trobridge G, Josephson NC, Russell DW (2001) Gene transfer into murine hematopoietic stem cells with helper-free foamy virus vectors. Blood 98: 604–609.
11. Josephson NC, Trobridge G, Russell DW (2004) Transduction of long-term and mobilized peripheral blood-derived NOD/SCID repopulating cells by foamy virus vectors. Hum Gene Ther 15: 87–92.
12. Leurs C, Jansen M, Pollok KE, Heinkelein M, Schmidt M, et al. (2003) Comparison of three retroviral vector systems for transduction of nonobese diabetic/severe combined immunodeficiency mice repopulating human CD34+ cord blood cells. Hum Gene Ther 14: 509–519.
13. Uchiyama T, Adriani M, Jagadeesh GJ, Paine A, Candotti F (2012) Foamy virus vector-mediated gene correction of a mouse model of Wiskott-Aldrich syndrome. Mol Ther 20: 1270–1279.
14. Bauer TR Jr, Allen JM, Hai M, Tuschong LM, Khan IF, et al. (2008) Successful treatment of canine leukocyte adhesion deficiency by foamy virus vectors. Nat Med 14: 93–97.
15. Si Y, Pulliam AC, Linka Y, Ciccone S, Leurs C, et al. (2008) Overnight transduction with foamyviral vectors restores the long-term repopulating activity of Fancc−/− stem cells. Blood 112: 4458–4465.
16. Morianos I, Siapati EK, Pongas G, Vassilopoulos G (2012) Comparative analysis of FV vectors with human alpha- or beta-globin gene regulatory elements for the correction of beta-thalassemia. Gene Ther 19: 303–311.
17. Chatziandreou I, Siapati EK, Vassilopoulos G (2011) Genetic correction of X-linked chronic granulomatous disease with novel foamy virus vectors. Exp Hematol 39: 643–652.
18. Trobridge G, Josephson N, Vassilopoulos G, Mac J, Russell DW (2002) Improved foamy virus vectors with minimal viral sequences. Mol Ther 6: 321–328.
19. Zhang F, Thornhill SI, Howe SJ, Ulaganathan M, Schambach A, et al. (2007) Lentiviral vectors containing an enhancer-less ubiquitously acting chromatin opening element (UCOE) provide highly reproducible and stable transgene expression in hematopoietic cells. Blood 110: 1448–1457.
20. Arima N, Kamio M, Imada K, Hori T, Hattori T, et al. (1992) Pseudo-high affinity interleukin 2 (IL-2) receptor lacks the third component that is essential for functional IL-2 binding and signaling. J Exp Med 176: 1265–1272.
21. Ishii N, Asao H, Kimura Y, Takeshita T, Nakamura M, et al. (1994) Impairment of ligand binding and growth signaling of mutant IL-2 receptor gamma-chains in patients with X-linked severe combined immunodeficiency. J Immunol 153: 1310–1317.
22. Asao H, Okuyama C, Kumaki S, Ishii N, Tsuchiya S, et al. (2001) Cutting edge: the common gamma-chain is an indispensable subunit of the IL-21 receptor complex. J Immunol 167: 1–5.
23. Ohbo K, Suda T, Hashiyama M, Mantani A, Ikebe M, et al. (1996) Modulation of hematopoiesis in mice with a truncated mutant of the interleukin-2 receptor gamma chain. Blood 87: 956–967.
24. Ito M, Hiramatsu H, Kobayashi K, Suzue K, Kawahata M, et al. (2002) NOD/SCID/gamma(c)(null) mouse: an excellent recipient mouse model for engraftment of human cells. Blood 100: 3175–3182.
25. Wu X, Li Y, Crise B, Burgess SM (2003) Transcription start regions in the human genome are favored targets for MLV integration. Science 300: 1749–1751.
26. Laufs S, Nagy KZ, Giordano FA, Hotz-Wagenblatt A, Zeller WJ, et al. (2004) Insertion of retroviral vectors in NOD/SCID repopulating human peripheral blood progenitor cells occurs preferentially in the vicinity of transcription start regions and in introns. Mol Ther 10: 874–881.
27. Montini E, Cesana D, Schmidt M, Sanvito F, Ponzoni M, et al. (2006) Hematopoietic stem cell gene transfer in a tumor-prone mouse model uncovers low genotoxicity of lentiviral vector integration. Nat Biotechnol 24: 687–696.
28. Trobridge GD, Miller DG, Jacobs MA, Allen JM, Kiem HP, et al. (2006) Foamy virus vector integration sites in normal human cells. Proc Natl Acad Sci U S A 103: 1498–1503.
29. Beard BC, Keyser KA, Trobridge GD, Peterson LJ, Miller DG, et al. (2007) Unique integration profiles in a canine model of long-term repopulating cells transduced with gammaretrovirus, lentivirus, or foamy virus. Hum Gene Ther 18: 423–434.
30. Hacein-Bey-Abina S, Garrigue A, Wang GP, Soulier J, Lim A, et al. (2008) Insertional oncogenesis in 4 patients after retrovirus-mediated gene therapy of SCID-X1. J Clin Invest 118: 3132–3142.
31. Zhu N, Gu L, Findley HW, Chen C, Dong JT, et al. (2006) KLF5 Interacts with p53 in regulating survivin expression in acute lymphoblastic leukemia. J Biol Chem 281: 14711–14718.
32. Ito T, Kwon HY, Zimdahl B, Congdon KL, Blum J, et al. (2010) Regulation of myeloid leukaemia by the cell-fate determinant Musashi. Nature 466: 765–768.
33. Stam RW, den Boer ML, Passier MM, Janka-Schaub GE, Sallan SE, et al. (2006) Silencing of the tumor suppressor gene FHIT is highly characteristic for MLL gene rearranged infant acute lymphoblastic leukemia. Leukemia 20: 264–271.
34. Huston MW, van Til NP, Visser TP, Arshad S, Brugman MH, et al. (2011) Correction of murine SCID-X1 by lentiviral gene therapy using a codon-optimized IL2RG gene and minimal pretransplant conditioning. Mol Ther 19: 1867–1877.
35. Otsu M, Sugamura K, Candotti F (2000) In vivo competitive studies between normal and common gamma chain-defective bone marrow cells: implications for gene therapy. Hum Gene Ther 11: 2051–2056.
36. Otsu M, Sugamura K, Candotti F (2001) Lack of dominant-negative effects of a truncated gamma(c) on retroviral-mediated gene correction of immunodeficient mice. Blood 97: 1618–1624.
37. Kume A, Koremoto M, Mizukami H, Okada T, Hanazono Y, et al. (2002) Selective growth advantage of wild-type lymphocytes in X-linked SCID recipients. Bone Marrow Transplant 30: 113–118.

Available online at www.sciencedirect.com

ScienceDirect

Current Opinion in Immunology

Molecular determinants of sterile inflammation

Hajime Kono, Akiko Onda and Tamiko Yanagida

Necrotic cell death alerts the acquired immune system to activate naïve T cells even in the absence of non-self derived molecules (e.g. pathogens). In addition, sterile necrosis leads to innate immune-mediated acute inflammation. The dying cells still represent a threat to the body that should be eliminated by the host immune response. Although the inflammatory response plays important roles in protecting the host and repairing tissues, it can also cause the collateral damage to normal tissues that underlies disease pathogenesis. Tissue resident macrophages recognize the danger signals released from necrotic cells via the pattern recognition receptors and secrete IL-1 that results in acute neutrophilic inflammation. This article will review our current knowledge especially focusing on the role of IL-1 in the sterile necrotic cell death induced inflammation.

Addresses
Department of Internal Medicine, Teikyo University School of Medicine, Kaga 2-11-1, Itabashi-ku, Tokyo 173-8605, Japan

Corresponding author: Kono, Hajime (kono@med.teikyo-u.ac.jp)

Current Opinion in Immunology 2014, **26**:147–156

This review comes from a themed issue on **Innate immunity**

Edited by **Seth L Masters** and **Dominic De Nardo**

http://dx.doi.org/10.1016/j.coi.2013.12.004

Introduction

The immune system can differentiate among forms of cell death and respond to a perceived threat accordingly. Unlike apoptosis, necrotic cell death induces an acute inflammatory response, even in the absence of pathogens. The innate immune system can sense changes in the integrity of the body. For example, sterile physical damage, such as a burn or bruise, evokes acute inflammation, which consists of the four canonical signs of inflammation: rubor (redness), dolor (pain), calor (heat), and tumor (swelling). These signs were described as early as 2700 years ago. By contrast to the longstanding recognition of the role of inflammation in sterile cell death, our understanding of the mechanism underlying this inflammatory response is just emerging [1–3]. One of the most important steps in this has been the identification of the key mediator interleukin 1 (IL-1) [4••]. Of the 11 members of the IL-1 family, IL-1α and IL-1β has been shown to be responsible for mediating the inflammatory responses to sterile cell death, whereas the IL-1R antagonist (IL-1Ra) is a physiological inhibitor of IL-1. All of IL-1α, IL-1β, and the IL-1Ra bind to IL-1RI signaling receptor which recruits adaptor protein Myd88 and culminated in NF-κB-induced transcription of inflammatory genes. IL-1α is preformed as a active molecule without further modification in cells mainly works as a membrane bound molecule [5]. IL-1β is not expressed under normal homeostatic conditions by bone marrow-derived myeloid cells and is induced as an inactive form by various inflammatory stimuli. Generation and secretion of active IL-1β as well as secretion of IL-1α are mediated by caspase-1 activation on the inflammasome [6••,7].

The mechanism leading to IL-1 production, inflammasome formation, is shared by a variety of stimuli, ranging from sterile stimuli such as dead cells and particulates to microbial stimuli such as bacteria, fungi, or viruses [7]. Although the final 4 canonical signs of inflammation is identical for infectious and sterile causes, the processes of responses to the various stimuli are diverse. Regarding the relationship between cell death and inflammation, apoptosis is a non-inflammatory programmed cell death which is a necessary part of development and tissue homeostasis to remove unwanted cells. Necrosis (oncosis) is an inflammatory non-programmed cell death, which is caused by passive disruption of the plasma membrane that results in releasing of the cytosolic contents to the extracellular space. Other than necrosis, macrophages and dendritic cells undergo an inflammatory programmed cell death, named pyroptosis, that is distinct from apoptosis and necrosis [8]. Pyroptosis is a lytic cell death and mediated by caspase-1 and inflammasome, while apoptosis is non-lytic and mediated by caspase 3/6/7 and apoptosome. Pyroptosis is inflammatory by releasing IL-1 family molecules and other cytosolic contents. More importantly, inflammation caused by necrosis is mediated and/or amplified by macrophages which sometimes undergo pyroptosis. This review focuses on inflammation triggered by sterile dead cells, and specifically on the molecular and cellular mechanisms of both IL-1α and IL-1β.

Danger theory and its extension to acute inflammation

Janeway proposed the principle of discriminating self from non-self by utilizing the recognition of conserved molecular patterns of pathogens, called pathogen-associated molecular patterns or PAMPs (Figure 1) [9]. In this theory, antigen-presenting cells can present the appropriate pathogen-derived peptide to and activate naïve T cells in the presence of PAMPs. This theory was confirmed by identifying Toll-like receptors (TLRs) as the PAMP receptors. TLR engagement on antigen

presenting cells indirectly enhances activated T cell proliferation, differentiation, and survival by promoting the up-regulation of costimulatory molecules and the secretion of proinflammatory cytokines. Nevertheless, this 'Stranger theory' cannot explain some of the well-known immune responses, including the sterile organ transplantation response. Matzinger proposed a theoretical answer to this question, named the 'Danger model' [10]. She explained how the immune system can recognize damage to self by sensing a 'Danger signal'. Danger signals are also capable of activating dendritic cells, which results in the activation of naïve T cells in the same manner as with PAMPs. This theory was confirmed by several studies in which dead cells promoted CD4+ and CD8+ T cell responses [11,12]. The original notion of danger theory was expanded to acute inflammation. TLRs and Nod-like receptors were characterized as pattern recognition receptors, which sense PAMPs and induce acute inflammatory responses [13]. When cells die *in vivo*, neutrophils and monocytes infiltrate the site [14]. This phenomena is also observed in the absence of pathogens; that is, under sterile conditions [15]. The precise mechanism that senses own cell death and induces inflammation was not clear. Advances in the last decade have revealed the molecular identity of the danger signal and the receptors and amplifiers that play a role in this sterile cell death-induced inflammation.

Players in the recognition and amplification of cell-death-induced inflammation

Danger signals

A variety of danger signals have been identified and are classified into two categories on the basis of their actions: (1) molecules that are usually sequestered inside cells and released on necrotic cell death and (2) extracellular matrix, which exposes hidden molecular patterns when fragmented [16]. The hidden intracellular danger signals include uric acid, HMGB1, the myosin heavy chain, SAP130, S100 proteins, ATP, and nucleic acids including mitochondrial DNA [17] (Table 1). Cytokines such as IL-1α and IL-33 have also been identified as danger signals and are released passively from necrotic cells [18–20]. Fragments generated from hyaluronic acid, collagen, elastin, and laminin all stimulate inflammation [16].

Uric acid was the first endogenous molecule identified as functioning as a danger signal via the activation of dendritic cells and enhances the CD8+ T cell responses *in vivo* [21•]. Later uric acid is shown to mediate acute neutrophilic inflammation to necrotic cells in the acute inflammatory responses to the injection of necrotic thymocyte cells or in acetaminophen-induced liver toxicity [22]. Uric acid also stimulates sterile-injury-derived inflammation in the lung [23] or kidney [24]. Uric acid is the end product of the cellular catabolism of purines, and present at near-saturating levels in body fluids and at much higher concentrations in the cytoplasm of cells. In addition, uric acid is produced after cell death by xanthine oxidase [21•,22]. It is speculated that production of uric acid from necrotic cells leads to the phase transition from soluble uric acid to urate crystals (i.e. monosodium urate crystal) around the dying cells with the high sodium extracellular milieu, although the formation of the crystals has not been proven *in vivo*. Monosodium urate (MSU) crystal is formed in human joints which causes acute gouty arthritis [25]. MSU crystals also have been shown to both activate dendritic cells and augment immune responses [21•]. MSU crystals, but not uric acid, induces chemokines and cytokines when added to eosinophils [26]. Collectively, MSU crystals rather than uric acid are the danger signals that can mount both of innate and adaptive immune responses in response to cell death.

Another prototype inflammatory danger signal is HMGB1 protein [27•]. In the normal setting, HMGB1 functions as a chromatin-binding nuclear factor, but it can also be actively secreted by activated immune cells and initiate inflammatory responses [28,29]. HMGB1 is passively released from necrotic cells; by contrast, apoptotic cells modify their chromatin so that HMGB1 binds tightly and thus is not released [27•]. Initially HMGB1 was reported to exert a cytokine like activity including release of TNF-α, IL-1α and IL-β, IL-1Ra, IL-6, IL-8, and MIP-1α and MIP-β when added to mononuclear cells [30]. Later it was shown that recombinant HMGB1 itself induce little or no cytokine secretion [31–33]. At this point, it is shown that HMGB1 forms complex with other molecules including ssDNA, LPS, IL-1β and nucleosomes and exerts inflammatory properties [29]. HMGB1 contributes to evoking inflammation in response to cell death in the sterile liver toxicity model [27•].

Mitochondria is a rich source of danger signals, including mitochondrial DNA, formyl peptides, cytochrome C, and ATP. The highly concentrated danger signals make mitochondria potent stimulators of inflammation [34].

IL-1α also functions as a primary danger signal in certain settings, including the death of dendritic cells or vascular smooth muscle cell [18,35,36]. We confirmed that the necrotic dendritic cells from IL-1α-deficient mice induced reduced inflammation when injected into the peritoneum, compared with cells from wild-type mice [37]. However, necrotic tissue from the liver, brain, and heart of IL-1α-deficient mice had a similar neutrophilic response [37]. Zheng *et al.* also showed the necrosis-induced IL-1α inflammatory activity is highly cell type dependent, and further revealed the molecular mechanism which regulates the activity of IL-1α when released from necrotic tissue [38•]. A decoy IL-1R type II (IL-1R2) which constitutively associates with cytosolic IL-1α and prevents its interaction with IL-1R1 upon release from necrotic cells. Moreover the active caspase-1 cleaves IL-1R2 to make IL-1α accessible to IL-1R1 in

Table 1

Intracellular danger signals, receptors and their biological effects *in vitro* and *in vivo*.

Danger signal	Putative receptor	Biological effect *in vitro*	Biological effect *in vivo*	Related pathologies in human
HMGB1	RAGE [89,90]	Chemotaxis [91] Cytokine induction [92] Macrophage activation [92] DC activation [93,94] Endothelial cell activation [95]	Antitumor immunity promotion [93,96] Liver injury [27•,97] Arthritis [98] Heart ischemia [90] Brain ischemia [99,100] Aortic aneurysm [101]	Sepsis [102] Brain ischemia [99] Aortic aneurysm [101]
Uric acid (MSU)	Cholesterol of plasma membrane [70] TLR2&4 [103] NOT TLR2&4 [73] CD14 [104]	Cytokine production [26,72] DC/MP activation [21•,72] Th17 differentiation [105] Chemotaxis & degranulation of eosinophil [26]	Liver injury [22] Adjuvant activity [21•] Neutrophil recruitment [22] Bleomycin induced lung injury [23]	Gout [106,107] Tumor lysis syndrome [108] Osteoarthritis [109]
Histone/nucleosome/ chromatin/DNA/RNA	TLR2&4 [110] TLR9 [86,111,112] RAGE [113] RIG-I family members [114] TLR3 [115]	Cytokine induction [115,116] DC and MP activation [117,118] B cell and DC activation in forms of chromatin-IgG complex [111,112] Neutrophil activation [119] Endothelial cell death [120] Complement factor B production [121] NF-κB activation [113]	DC maturation [117,118] Liver injury [86,110] Sepsis [120,122] Neutrophil recruitment [113] Sunburn [115]	Systemic lupus erythematosus Sepsis [120]
ATP	P2X and P2Y receptors [123]	Inflammasome activation [124] Chemotaxis [125] Cytokine production [26]	Neutrophil recruitment [43]	
Adenosine	P1 receptors (A2A) [47•,48,61,123]	Suppression of cytokine induction [61]	Protection of liver injury [47•,48]	
SAP130	Clec4e (Mincle) [65•]	Cytokein and chmokine production [65•]	Nerutrophil recruitment [65•]	
Actin filaments	Clac9a (DNGR-1) [68,69]	Cross presentation [66•] Divert necrotic cell cargo into a recycling endosomal compartment [67]	Cross presentation [66•,63,67]	
Non-muscle myosin heavy chains (type IIA and C)	Natural IgM [126]	Activation of complements [127]	Ischemia of heart, muscle and intestine [128,129]	
Mitochondria *N*-formyl peptides	FPR1 [130]	Chemotaxis [131] Cytokine production [43,132]	Neutrophil recruitment [43,133] SIRS [134•] Liver injury [135]	
Mitochondria DNA/ mitochondrial transcription factor A	TLR9 [134•,136,137] RAGE [137]	Type I IFN production [137] Cytokine production [134•]	Neutrophil recruitment [134•] SIRS [134•] Dilated cardiomyopathy [136]	
Peroxideroxin	TLR2&4 [100]	IL-23 production [100]	Brain ischemia [100]	
IL-1α	IL-1R1 [7]	Cytokine production [35,38•] Chemikine production [18,35]	Neutrophil recruitment [18,37,38•]	
IL-33	IL-1RL1(ST2) [39]	Cytokine production [19,20]	Neutrophil rectuitment [19,39] Allergic airway inflammation & Colitis [138]	

addition to its known role in secreting IL-1α. Therefore, IL-1α from necrotic cells contributes to neutrophilic inflammation as a primary danger signal; although this is not always true and appears to be cell type dependent. IL-1α also serves as an indispensable second messenger actively secreted from macrophages which receives danger signals (see below section [Sensor cells for danger signals that generate IL-1]). IL-33 is also released from dead fibroblasts and provokes an inflammatory response [20,39].

Figure 1

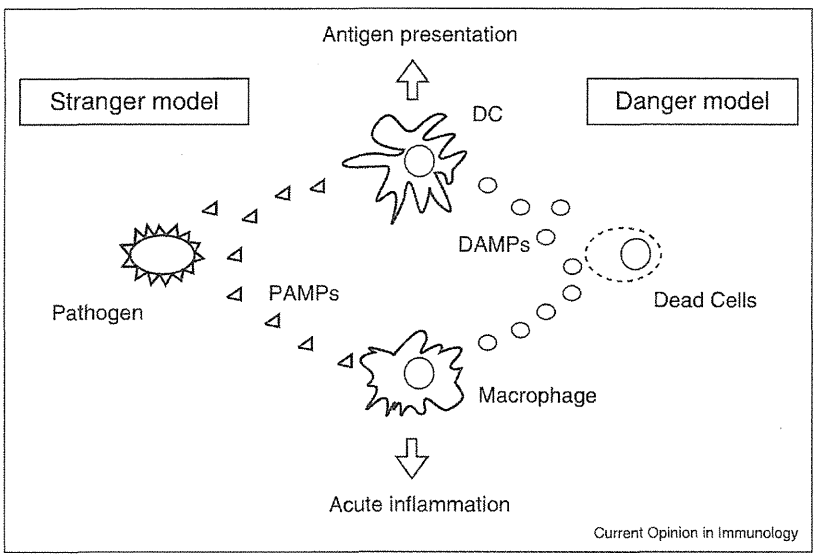

Stranger and danger models. To discriminate self and non-self, dendritic cells require an appropriate signal to be activated. Dendritic cells recognize pathogen associated molecular patterns (PAMPs) released from pathogens and get activated to present pathogen derived peptide to naïve T cells (Stranger model). Dendritic cells also recognizes danger signal or damage associated molecular patterns (DAMPs) released from necrotic cells and initiate the antigen presentation (Danger model). These models are applied to the acute inflammatory response in macrophages in response to PAMPs and DAMPs.

Extracellular ATP is a prototype inflammasome activator; it engages the P2X7 ATP-gated ion channel, triggering a K^+ efflux and inducing the gradual recruitment of pannexin-1 membrane pores [40,41]. ATP is released upon necrotic cell death and induces inflammation *in vivo* [42,43]. ATP is also released upon apoptotic cell death and works as a 'find-me' signals that recruit motile phagocytes, leading to the prompt clearance of the dying cells [44•]. They indicated that early apoptotic cells release very small amounts of ATP (<2% of intracellular ATP), which should be much less and could be distinguished from necrotic cells that may release much of their ATP content [45]. Intriguingly, adenosine is also released from necrotic cells but identified as an immunoregulatory danger signal that limit the excessive collateral tissue damage [46,47•,48].

Ligands for C-type lectin receptors including SAP130 or filamentous actin were identified as danger signals. These are described in section [Danger signal receptors] below.

As stated above, neutralization of HMGB1 reduces cell death induced liver toxicity. On the other hand, necrotic mutant fibroblasts lacking HMGB1 are as proinflammatory as wild-type fibroblasts when injected into murine peritoneum [4,27•]. Therefore, there is redundancy in danger signals *in vivo*, which makes it difficult to evaluate the roles of each. As such, the dominant danger signal varies in the context of the sterile injury, including the location (organ, tissue or region), magnitude, manner of cell death, and time point after the insult. Matzinger also suggested that the tissue influences the outcome of the immune responses to a large extent [49].

Receptors for danger signals

It was speculated that the two major stimuli of inflammation, infection and sterile injury, also share recognition pathways. In infections, TLRs recognize microbial components and stimulate inflammation via the activation of transcription factors NF-κB or interferon regulatory factors (IRFs), and the expression of proinflammatory cytokines [50,51]. Chen *et al.* examined the role of each TLR using the *in vivo* model of peritoneal inflammation in response to necrotic cells. The inflammation was reduced modestly in TLR2 and TLR4 double-deficient mice, but not in mice deficient only in each individual TLR (TLR1, 2, 3, 4, 6, 7, 9, and 11) [4••]. TLRs signal via one or more different intracellular TIR adaptor molecules: MyD88, TIRAP/Mal, TRIF, and TRAM. The inflammatory response to dead cells was reduced greatly in mice lacking MyD88, but not TIRAP/Mal or TRIF. The IL-1 receptor, which also utilizes MyD88, was identified as playing a major role in sterile inflammation in response to dead cells [4••]. The IL-1 receptor recognizes both IL-1α and IL-1β. IL-1α serves as a primary danger signal from dead cells in certain settings, as described above. IL-33 also